FACULTY OF SCIENCE AND TECHNOLOGY

MASTER'S THESIS

Study programme/specialization: Drilling Technology	Spring semester, 2017 Open
Author: Mats Rasmussen	.... (signature of author)
Programme coordinator: Supervisor(s): Mohsen Assadi, Alireza Zare	
Title of master's thesis: Impact of Well Configuration on CO_2 Injection for Energy Exploitation in Geothermal/Geopressured Reservoirs	
Credits: 30	
Keywords: Aquifer, dissolved CO_2, geothermal, well configuration simulation	Number of pages: 43 + supplemental material/other: 9 Stavanger, 15/06/2017

Title page for Master's Thesis
Faculty of Science and Technology

Acknowledgements

Abstract

Injecting dissolved CO_2 into deep saline aquifers is one of the more promising methods of alleviating greenhouse gas emissions. By simultaneously extracting the geothermally-heated brine in the aquifer, there is an opportunity to offset the energy consumption required by carbon capture and storage. This study uses a simulation tool to explore the effect of well placement on CO_2-storing efficiency. Eight models with different well configurations were tried on a homogeneous aquifer. The study found that storing efficiency was heavily reliant on distance, especially vertical, between the wells and the vertical-to horizontal permeability ratio. For a given aquifer model, there exists a depth differential between wells that optimize injection- and production rates versus gas-breakthrough time.

Contents

List of Figures

List of Tables

1 Background of the thesis

Carbon dioxide, or CO_2, emissions from the fossil fuel industry and power plants, contributing to global warming, have spawned a number of techniques to counteract the unnatural high levels of CO_2 in the atmosphere. The main goal behind these techniques is to store CO_2 and other types of carbon, indefinitely hopefully, in locations where they cannot interact with the atmosphere. As such, carbon capture and storage (CCS) utilizes different forms of underground storage. Depleted oil and gas reservoirs, un-minable coal beds and deep saline aquifers offer the most convenient means of large-scale CO_2 storage [1].

In this thesis, deep saline aquifers will occupy the focal point of the investigation. Furthermore, aquifers containing methane-brine. Many studies have been done on different types CO_2 sequestration. One of the more efficient ways of storing CO_2 discovered, is to dissolve the gas in brine and then inject it into an aquifer. If you have a production well in addition to your injection well, the brine with dissolved CO_2 can displace the methane- brine, replacing a methane-filled, geothermally-heated brine with an unwanted CO_2-filled brine. The win-win scenario produces a fluid which can be exploited for its heat and gas content.

One of the reasons using CO_2-brine is beneficial, has to do with the increased energy withdrawal possible compared to when using supercritical CO_2 as an injection fluid. The energy withdrawal potential residing in the use of brine, has to do with the brine's mobility in the formation. Another benefit of using brine to displace brine has to do with the compressibility factor. Displacing, and ultimately replacing, a fluid with another fluid of negligible compressibility discrepancies, causes less tampering with in-situ geological pressure regimes. This is advantageous for the long-term storing aspect of this process, decreasing the chances of a potential leak [2] [3].

1.1 Objective of the thesis

Using computer simulation tools, this thesis aims to look at different well placements and configurations and their effect on CO_2-storing efficiency in a deep saline aquifer. Additionally, the effect of the different well scenarios will be investigated regarding produced fluid and temperature distribution in the aquifer. Finally, aquifer parameters, e.g. permeability and thickness, will be varied to see their effect on the well scenarios.

1.2 Structure of the thesis

Chapter 2 contains information regarding the overall process of CCS. The chapter includes methods of capturing carbon, how it is transported to its designated location and the intricacies of well design, among other subjects relevant in the understanding of the CSS process as a whole. Chapter 3 reviews different papers published on topics similar to the objective of this thesis. Chapter 4 comprises the simulation part of this thesis with assumptions and results, and reviews requirements put on a system for the simulator to work. Chapter 4 also takes into consideration other thermodynamic relations that exist when extracting geothermal fluids from the earth. Chapter 5 contains discussion regarding results from chapter 4. The conclusion of the thesis is found in chapter 6.

2 A technical perspective

The world's power stations – including oil refineries and petrochemical plants - produce massive amounts of CO_2 every day. But there is a benefit of having the CO_2 emissions be concentrated: they can be, more easily, captured and stored. That is what is being done today around the world. Although, the different technologies available need to be implemented on a large scale to have an impact.

2.1 Capturing gas emissions

There are methods of capturing the CO_2 from the exhaust gas, known as flue gas, produced at the power stations post-combustion. One of them is to bubble the flue gas through a solvent, making the solvent react and absorb the CO_2. This method makes power plants 20% less efficient, but renders them almost carbon neutral – more than 90% of the CO_2 in flue gas can be captured. Another possibility is membrane separation, where CO_2 either passes through a membrane or remains. The separated CO_2 can be treated, chemically or physically, in various ways to capture it.

In coal-burning power plants, CO_2 can also be captured pre-combustion. This can be achieved if the coal is put through a gasifier where it partially oxidizes and creates CO and CO_2. When the coal is ultimately put in a boiler, the flue gas can be made more CO_2 rich by burning the coal in an oxygen-rich atmosphere – making the other unwanted components of the flue gas less prominent.

After the CO_2 has been successfully captured, it needs to be transported to its target location. In the US, there are more than 3900km of pipelines, made for CO_2 transportation. Most of the CO_2 is injected into old oil fields. In this thesis however, deep saline aquifers will be the focal point. Keeping in mind that water is incompressible and that a typical reservoir takes on an anticlinal shape, when we displace brine with brine, the contents of the saline aquifer have to go somewhere. If the aquifer is a closed system, pressure build-up exceeding lithostatic pressure would cause the sealing rock, or cap rock, to fracture. Meaning you could not store as much CO_2 as the aquifer volume would suggest. If the aquifer is an open system, the initial contents would spill out into other structures, or even rise to the surface. At the Sleipner field, off the coast of Norway, they started CO_2 injection, in 1996, into the Utsira Sand. This deep saline aquifer does not have a typical anticlinal trap, or seal, shape. However, the Utsira Sand is incredibly large and has a cap rock confining it. In this thesis, we are looking to exploit the displaced brine for geothermal energy, as well as making use of its methane content.

When storing CO_2 deep underground, one would typically want to inject CO_2 into the reservoir in its supercritical state. For CO_2, this would mean a temperature and pressure exceeding 31.1°C and 73.8bar. When reaching this state, CO_2 has a higher density than it would under normal surface conditions. A sufficient density increase makes the CO_2 occupy only a quarter of 1% of its original volume [1].
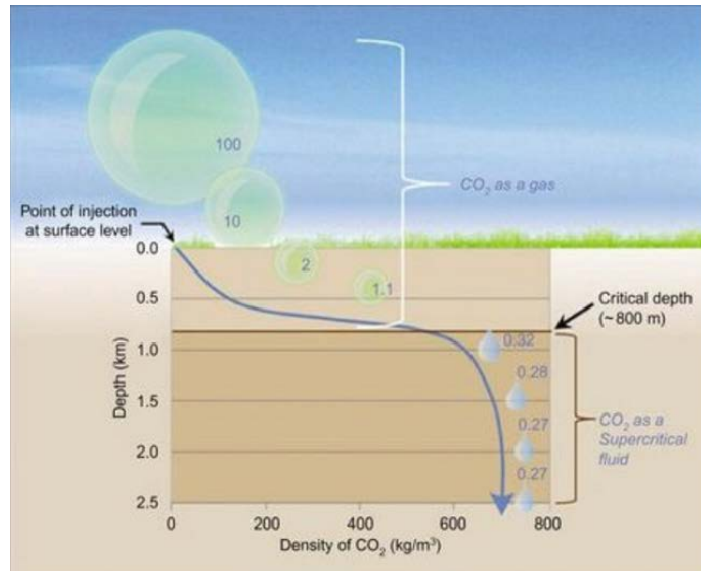
Figure 2.1: Showing the effect of pressure on CO2 density [1].

2.2 Stability of stored CO2

CO_2 can remain trapped underground for millions of years. In ca. 1960, Shell made a discovery in Jackson, Mississippi. They found 200 million tonnes of natural CO_2. The accumulation is trapped under a huge anticlinal shape of cap rock. It is buried approximately 5km underground, which makes the CO_2 assume a supercritical state. By using well established dating methods, scientists were able to determine the age of the CO_2 to be approximately 70 million years old.

When injecting and storing CO_2 in a deep saline aquifer, there is a chance of the supercritical CO_2 moving a certain distance over time. But, the entirety of the CO_2 volume does not move – residual amounts are left behind in the rock pores. That means, if the aquifer is big enough, the volume of supercritical CO_2 moving would bleed off until it reached a volume equal to the residual volume the rock pores could contain. This method of trapping CO_2 is called 'hydrodynamic trapping' and does not require a seal rock or an anticlinal shaped aquifer.

CO_2 is a reactive gas and can react with pore water and with certain rock particles. If CO_2 dissolves in pore water, it loses its buoyancy and behaves similarly to supercritical CO_2 being hydronamically trapped, keeping the CO_2 in the reservoir. This 'solubility trapping' is the principle behind what we are looking at in this thesis. However, we want to inject a brine with CO_2 already dissolved in it at the surface. The solubility of CO_2 in brine increases with increasing pressure, but decreases as temperature and salinity increases [1].

3
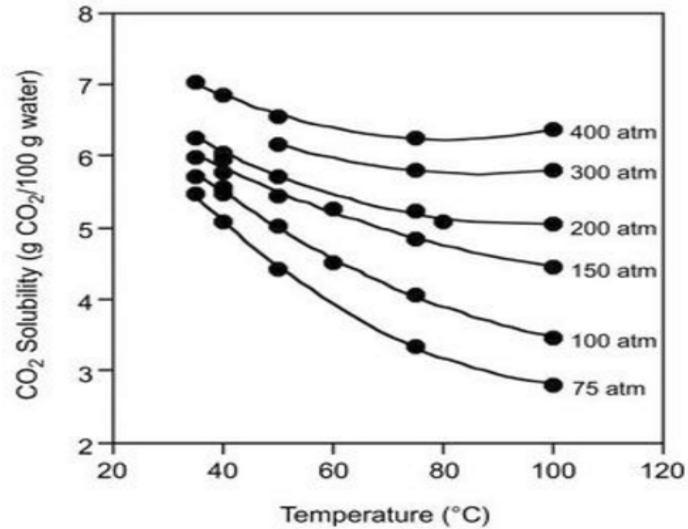
Figure 2.2: Temperature effect on CO2 solubility at different pressures [1].

When CO_2 dissolves in water, it forms a weak acid. The acid may further react with the rock and form new minerals. This method of trapping is called 'mineral trapping' and although it is beneficial to fix the CO_2 to the rock in this way, scientists are not yet certain of reaction times regarding mineral trapping.

Dissolving CO_2 in saline water makes the brine denser than pore water. The denser brine will then sink rather than rise compared to the pore water. This effect should be taken into consideration regarding well placement. In the simulation part of this thesis, non-chalk aquifers will constitute the investigation regarding aquifer type. The reason for this choice has to do with storage space. There was a fairly recent study presented in 2012 on storage space of offshore Britain. The study was called United Kingdom Storage Appraisal Project (UKSAP), and without going into too much detail, they concluded that a total of 78 gigatonnes of CO_2 could potentially be stored in the North Sea, some of it in the Irish Sea and English Channel. 60 gigatonnes, approximately 77% of the total volume, is courtesy of deep saline aquifers made of sandstone.

Wealthy countries like USA, UK, Norway, and Germany etc. are contributing to global warming, but they are doing - and have the technical ability to do - something about their emissions. Emerging countries like China and India have an incredibly high consummation of coal currently. It is therefore vital that they partake in the fairly new practice of CCS. This means resources need to be poured into researching, most importantly due to storage capacity, deep saline aquifers. For practical purposes, the aquifers should be close to the power plant clusters - where power plants exist in higher density. Or, future power plants being built need to have the aquifers' locations in mind [1].

2.3   Likelihood of CO_2 leakage

If CO_2 has been artificially stored underground in either a deep saline aquifer or an old depleted hydrocarbon field, what are the chances of the CO_2 leaking upwards towards the surface? As time goes by, the CO_2 becomes more stable as it reacts with pore water or certain rock minerals. But there are still ways for the CO_2 to escape before having assumed these stable forms. Preferably, you want to use already-drilled wells for the CO_2 injection to save costs. If there are abandoned oil or gas wells nearby, they might act as migration pathways for the CO_2. Abandoned wells, on the Norwegian continental shelf, shall follow strict rules and regulations as stipulated by the NORSOK D-010 standard. Even though the standard ensures well integrity, anomalies can occur. Another way for the CO_2 to escape can be through permeable faults in a supposed impermeable formation. Also, previously impermeable faults may change when a reservoir is pressurized.
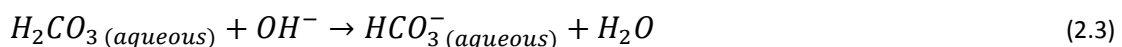
These are all reasons why storing CO_2 artificially should be done using CO_2-brine rather than supercritical CO_2. The reservoir pressure will be kept, more or less, constant using brine to displace brine, limiting fault interference. Also, using brine negates the buoyancy effect that would otherwise be present if using supercritical CO_2 – the brine will sink. Furthermore, since scientists are uncertain about reaction times regarding CO_2 and pore water, injecting CO_2-brine eliminates this aspect of storing [1].

Before reviewing papers on CO_2-brine injection, we will look at how the CO_2-brine can be manufactured and its costs, concluding the justification for CO_2 brine use.

2.4   Carbonated brine and chemistry

Mixing CO_2 into the brine is done at the surface. This process requires a pressure put on the brine and captured CO_2. As mentioned earlier, solubility increases as pressure increases. The mixing rate also increases with increasing pressure - when injecting the fluids into the mixing vessel, the fluids need to reside within the vessel for a certain amount of time for the process to complete. Studies show a pressure of approximately 75bar can make that happen in 4 minutes. As solubility decreases with temperature increase, relatively low temperatures are used for the fluids (approximately 30°C for the CO_2 and 22°C for the brine). The rates at which CO_2 and brine is injected into the vessel for mixing also have to be managed respectively for fairly obvious reasons. If either one of the fluids are injected too fast or too slow, you will not obtain maximum efficiency and costs will be higher. Additionally, increasing salinity decreases the solubility. Because of the aforementioned reasons regarding pressure, temperature and salinity, the brine will typically need to be injected at a higher rate than the CO_2. The SPE paper, 'CO_2-Brine Surface Dissolution and Injection: CO_2 Storage Enhancement', studied the dissolution rate with a simulator and found that, when using the abovementioned pressure and temperatures, depending on the brine salinity, the rate at which the brine had to be injected into the vessel needed to be two to ten times higher than that of the CO_2 injection rate [4].

The chemical reactions that happen when CO_2 react with water may be described in the following way:

$$CO_{2\,(gaseous)} \rightarrow CO_{2\,(aqueous)} \tag{2.1}$$

$$CO_{2\,(aqueous)} + H_2O \rightarrow H_2CO_{3\,(aqueous)} \tag{2.2}$$

$$H_2CO_{3\,(aqueous)} + OH^- \rightarrow HCO_{3\,(aqueous)}^- + H_2O \tag{2.3}$$

In equation (2.3), carbonic acid reacts with OH^- and forms so-called bicarbonate and water. This reaction is the solubility trapping mechanism [4].
The ionic trapping mechanism is may be expressed as:

$$HCO_{3\ (aqueous)}^- + OH^- \rightarrow CO_{3\ (aqueous)}^{-2} + H_2O \tag{2.4}$$
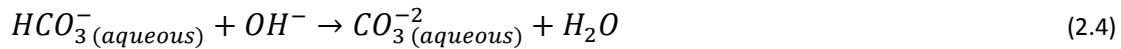
Lastly, mineral trapping may be expressed as:

$$CO_{3\ (aqueous)}^{-2} + Ca^{2+} \rightarrow CaCO_{3\ (solid)} \tag{2.5}$$

Equations (2.1), (2.2), (2.3), (2.4) and (2.5) were taken from 'CO₂-Brine Surface Dissolution and Injection: CO₂ Storage Enhancement' [4].

There are also the mixing vessel specifications to consider. Is it better to use one large mixing vessel, or a higher number of smaller units? Costs and convenience might influence your choice. The 'ASME Boiler and Pressure Vessel Code' gives design guidelines fo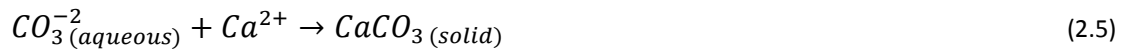r pressure mixing vessel. Pressure is an important factor in the mixing process and the code ensures safety. The code governs the design, fabrication and inspection of boilers and pressure vessels [5].
Furthermore, the pressure of the injection fluid, i.e. the carbonated brine, should equal the wellhead pressure. The wellhead, if offshore, will usually sit on the seafloor. It provides pressure control and a framework for all the casings to hang off. The casings help ensure stability of the wellbore against the formation. Additionally, the wellhead provides a framework where you can mount your surface flow-control equipment, i.e. Christmas Tree or Blowout Preventor (BOP). If you are using a 'Vertical Christmas Tree', the tubing hanger will sit inside the wellhead (if you are using a 'Horizontal Christmas Tree', the tubing hanger is inside the Tree). The tubing hanger is where your tubing hangs off. The tubing, or 'Coiled Tubing', lets you, among other things, circulate fluid into your wellbore.

2.5   Carbonated brine and physics

The wellhead pressure will depend upon the reservoir pore pressure. If there is no pressure in your well and a connection to the reservoir has been made, you will get an influx of reservoir fluid into your well. The connection to the reservoir is done using a 'perforation gun'. The gun utilizes explosive charges that perforate the casing and formation. To get the gun into the desired location where you want it to fire, a 'wireline' can be used. The wireline acts as a fishing pole and can be used to lower tools, among other operations, into your well. The pressure differential between the reservoir and your wellbore has to be managed somehow. If there is no pressure to counteract the pore pressure of the reservoir, the influx of fluids into your wellbore will cause a 'kick' at the surface. The kick, or sudden increase in fluid returns, can cause a blowout if your BOP fails. To neutralize the pressures of the formation acting on the wellbore, fluid is pumped into- and used to occupy the space inside your wellbore. The weight of the fluid column creates a 'hydrostatic pressure'. When drilling into the earth's crust, the deeper you go the higher the pressure gets. The pressure-increase due to the column of rock and fluids contained in the rock is higher than the pressure which would be generated at the bottom of a column of seawater - the so-called 'geostatic gradient' is higher than the hydrostatic gradient of seawater. Because the pressure increases more per unit length of rock versus seawater, a heavier fluid has to be used instead. The rock is also subject to compaction because of its compressibility. When the pressure increases with depth, the rock increases its density. This means that the geostatic gradient is increasing as you go deeper – it

does not remain constant. For this reason, and due to the fact that many fluids have low compressibilities, you need to change, or increase the density of, the fluid used for drilling as you drill deeper. The casings are therefore used to provide margins in which to operate. The casings help isolate the different sections of your wellbore before drilling deeper with a heavier fluid. Because the casing is set after drilling a section, you can only increase your fluid weight by so much. If too heavy a fluid is used, the formation will not be able to withstand the pressure created by the fluid column and fractures will propagate throughout the formation. When you are drilling, you want to operate within a safe window. That is, you do not want to exceed the fracture pressure of the particular formation, nor do you want to go below the pore pressure of that formation. If you end up fracturing your formation unintentionally, drilling fluid will escape your wellbore. When this happens, pressure previously generated by your fluid column will be lost and you will take a kick. As explained earlier, if the pressure generated by your fluid column is below the pore pressure, and the formation contains fluids, you will take a kick. Another outcome of too low a pressure in your wellbore, is that the wellbore will collapse. This can result in a stuck drillpipe.

To plan a safe working window for drilling a well, it is common practice to use a scheme, or well plan, like the one depicted in figure 3.
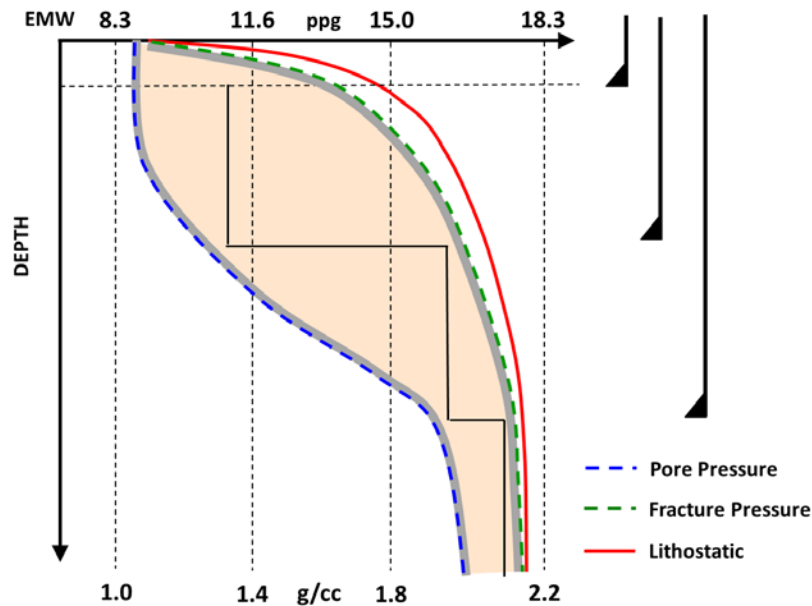
Figure 2.3: Plot of pore pressure and fracture pressure with depth [6].

Figure 3 shows a simplified version of how one would go about planning 'mudweight' and the different casing's placements. Mud is what the petroleum industry calls their drilling fluid. On the x-axis of figure 2.3 it says 'EMW', which is the equivalent mudweight. This means you need, here showing pounds per gallon (ppg) at the top and grams per cubic centimeter (g/cc) on the bottom, to use a certain density for your mud to stay within the safe working window. The safe working window would be the area colored a tan brown. The depth is shown on a negative y-axis for convenience's sake. Inside the working window there is a step-wise black line. The vertical sections of the black line show the mud density used for drilling to that depth. The horizontal part of the black line is where there has to be an increase in mud density to keep drilling safely. These steps of increased mudweight is also where there is a change in casings. Depicted to the right on figure 2.3, you can see at which depths the casings change

corresponding to the increase in mudweight. The casings themselves have to decrease in diameter as you drill deeper, similar to Russian nesting dolls. The casing on the bottom of your wellbore has a much smaller inner diameter than your top casing, or conductor casing. For this reason, the tools you lower into your well will often have their size determined by the thinnest section of your well. For instance, if you were to perforate the bottom casing, usually a 'production liner', the gun's dimensions would have to be scaled accordingly.

Bernt S. Aadnøy defined the 'median line principle'. The principle has to do with choosing mudweights that cause the least amount of disturbance to your wellbore. The median line follows what the average horizontal stress is in your formation. The average horizontal stress is therefore equal to the average pressure between the pore pressure and fracture pressure. This means the mudweight should be as close as possible to the in-situ stress field of the surrounding formation [7]. Without going into too much detail, following the method minimizes problems regarding differential sticking, lost circulation, tight hole and wellbore collapse. Differential sticking happens when there is a pressure differential between your wellbore and a permeable zone in the formation, with high pressure in your wellbore and lower pressure in the permeable zone, causing the drillstring to get stuck. When drilling through permeable zones, residue from your drilling fluid will be left behind there due to the higher pressure in your wellbore. The residue forms something the petroleum industry refers to as 'filter cake'. If the filter cake is present over a large area, the differential pressure between your wellbore and permeable zone need not be large for the drillpipe to get stuck. Meaning, you will not be able to continue drilling or pull your drillstring out of the hole without exceeding the yield strength of your steel drillpipe. Differential sticking is a common problem in the drilling business.
Tight hole is a less severe version of well collapse where the rock surrounding your wellbore yields and can cause stuck pipe. The rock yields due to high tangential stress in the wellbore. A reduction in hole diameter can also happen after drilling an area because of 'clay swelling'. Clay may exist in the formation and can react with drilling fluids causing an impermeable barrier along the wellbore.

The equations that govern stresses acting on the borehole may be expressed in the following way:

$$\sigma_r = P_w \tag{2.6}$$

$$\sigma_\theta = 2\sigma_a - P_w \tag{2.7}$$

$$\sigma_v = constant \tag{2.8}$$

In equation (2.6), σ_r is the radial stress and P_w is the pressure in the wellbore. In equation (2.7), σ_θ denotes the tangential stress, or hoop stress. σ_a is the average horizontal in-situ stress.

The wellbore reaches fracturing pressure when the effective hoop stress is zero, or $\sigma_\theta - P_o = 0$. Combining this fracturing pressure with equation (2.7) results in:

$$\sigma_a = \frac{1}{2}\left(P_{wf} + P_o\right) \tag{2.9}$$

P_{wf}, in equation (2.9), denotes the fracture pressure. The average between the pore pressure and the fracture pressure makes up the average horizontal stress in a wellbore [7].

When reaching your reservoir, there is a relatively rapid increase in pore pressure. The pressure increase has to do with impermeable rock cutting off the fluids in your reservoir from the fluid column they would otherwise form all the way to sea level. For instance, if there exists a connection between a fluid deep underground, through permeable rock, all the way to the seafloor, the pressure of the underground fluid would abide by equation (2.10). When there is a discontinuity in the fluid column, the fluids that have been caught beneath the impermeable rock cannot escape upwards and have to support the overlying rock layers. This is why reservoirs containing fluids have abnormally high pressures. It is also the reason why, when nearing or entering the reservoir zone, there is a much smaller gap between pore pressure and fracture pressure. The small difference in pore- and fracture pressure makes for a delicate operation. Inaccurate pore pressure estimations can cause your well to take a kick. When drilling high pressure high temperature (HPHT) wells, the difference between pore pressure and fracture pressure becomes even smaller. A HPHT well is a well that is deeper than 4000m, has a reservoir pressure exceeding 10 000psi and temperature exceeding 150°C [7]. Many wells in the Gulf of Mexico fall under this category, the Macondo well being one of them.

Hydrostatic pressure a column of fluid generates may be expressed in the following way:

$$P_{hyd} = \rho_{fluid}gD \tag{2.10}$$

ρ_{fluid} is the density of the fluid in the fluid column. g is the gravitational acceleration and D is the depth, or height, of the fluid column.

2.6   Conclusions

To summarize, the drilling procedure can be a very complex one and there are certain physical and chemical requirements drilling fluids need to fulfill. For these reasons, you would not use carbonated brine as your drilling fluid at any point. Therefore, you would need to use preexisting wells that have usable and accessible deep saline aquifers. Another option is to drill a new well for the intended purpose of CO_2 and/or carbonated brine injection. Of course, drilling a new well is not cheap. The U.S. Energy Information Administration (EIA) prepared a report on 'Trends in U.S. Oil and Natural Gas Upstream Costs' in 2016. As a disclaimer and by law, "... EIA's data, analyses, and forecasts are independent of approval by any other officer or employee of the United States Government. The views in this report therefore should not be construed as representing those of the Department of Energy or other federal agencies." [8]. Bearing this in mind, if the cost estimates are indeed in the same ballpark of actual costs, they should infer some idea as to whether drilling a new well would be economically beneficial. One should also consider the carbon footprint of drilling a new well. If the area in which the well is being drilled has the required aquifer, does the aquifer's storage capacity justify having drilled the new well? It begs the question that using preexisting wells would be the most likely scenario in which CSS is to be used.

Because of ever improving technologies and techniques, costs of all types of technologies, and how to implement them, decrease over time. According to EIA's analyses, drilling an onshore well in 2014 ranges in costs from $4.9 million to $8.4 million. These estimates include average completion costs ranging from $2.9 million to $5.6 million per well [8].

Offshore wells are drilled less frequently. In the Gulf of Mexico, less than 100 wells, including exploration and development drilling, are drilled each year. In comparison, several thousand are drilled

each year onshore USA. Nevertheless, time and capital invested in offshore wells is comparable. The reservoirs from which you retrieve hydrocarbons will vary in well productivity [8]. Each reservoir may contain hydrocarbons formed at different times in earth's history. It is fairly common knowledge that hydrocarbons naturally occur in crude oil [9] and that the oil is formed in the earth's crust under high pressure and high temperature. The material that is transformed into oil, or petroleum, is usually large quantities of algae [10] [9]. This transformation requires a very long time period, measured on a geological time scale. Over millions of years, when the algae get deposited in sedimentary rock, new layers of sediments bury the algae deeper and deeper. Sediments, which are made up of minerals and/or organic matter, settle in place to form sedimentary rock [11]. When the sediments get deep enough into the earth's crust without escaping, pressure and temperature can transform them into petroleum over time. What is not so common knowledge is that the different eras in which the algae was deposited, to later form petroleum, give rise to different well productivities. In the Gulf of Mexico, the well productivity is higher in reservoirs that are found to be from the Miocene era than ones found to be from the Jurassic era. Miocene wells cost approximately $120 million per well as of 2015. Jurassic wells cost approximately $230 million per well. The difference in well productivity has to do with water depth, well depth, pressure, temperature, and the geological features [8].

The reduced demand of fossil fuels in today's energy market may prompt a decommissioning of several wells, offshore and onshore, as they are no longer economically viable. Neither are they environmentally friendly, hence the reduction in demand. These abandoned wells, if deep saline aquifers are accessible from them, make for prime CSS candidates.

3 Review of papers related to carbonated brine sequestration

Before delving into the simulation part of the thesis, it would make sense to have a look at papers that have done similar studies and simulations and what their results were. The papers that have been taken into consideration, are ones that study the use of production wells to extract and exploit the geothermally heated fluid already present in the reservoir. If we assume a mass imbalance for extracted fluid to injected fluid, i.e. that the produced fluid has a higher rate than the injected fluid, the imbalance would cause a pressure drawdown in the reservoir. This drawdown would then help expedite the migration of carbonated brine into the reservoir and help regain mass balance and pressure equilibrium [4]. Because of this pressure effect, a mass balance of injected fluid to produced fluid is reasonable.

3.1 Offsetting costs of CCS

In 2014, Reza Ganjdanesh et al. published a paper called "Integrating carbon capture and storage with energy production from saline aquifers: A strategy to offset the energy cost of CCS" [2]. The study sought to estimate how much power one could generate from the extracted, geothermally heated, methane brine. The study also wanted to compare the power generation to the power consumption of CCS. Ganjdanesh and his team developed nine aquifer models, each representing a different depth. Because of the different depth intervals, each aquifer would have a unique power potential. The aquifer parameters were based on averages of conditions found in the Gulf of Mexico. The choice of parameter averages suggests offshore storing.

Looking at the power consumption of CCS, capturing and pressurizing the CO_2 is where most of the energy is spent. Using solvents for capturing the sour components, H2S and/or CO_2, of flue gas is a well-established method. The process of capturing and pressurizing CO_2 to a supercritical state by said method uses approximately 30% of a coal-fired power plant's energy output. Including the other drawbacks of injecting supercritical CO_2 into the aquifer, e.g. pressure build-up and CO_2 leakage, Ganjdanesh and his team opted for carbonated brine as their injection fluid. In addition to eliminating or mitigating the disadvantages of using supercritical CO_2, they found that the brine injection would enhance in-situ methane and geothermal energy recovery.

The simulation model used in the paper utilizes a horizontal well pattern. This pattern was used to increase production rate and sweep efficiency. It is a fairly logical placement of an injection- and a production well. The injector is placed deeper than the producer. The reason for this has to do with the injected brine being denser than the produced brine. The lighter brine will be displaced upward, although they found that gravity had little effect on the displacing process. Brine displacing brine also had a much higher sweep efficiency than gas displacing brine. The aquifer geometry used is represented by a prism shaped model. The shape has a symmetry to it which, one could argue, would describe a general case for brine displacing brine in a reservoir – regardless of reservoir type, the principles behind displacement remain the same. In which case, the well placements seem very sensible.
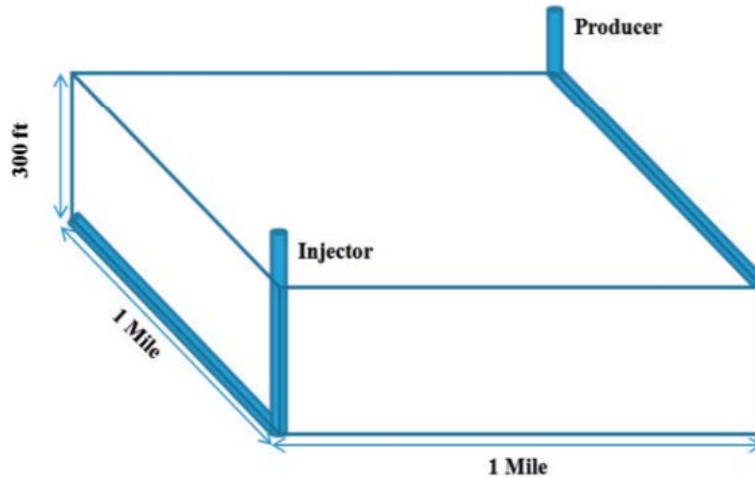
Figure 3.1: The simulation model used in "Integrating carbon capture and storage with energy production from saline aquifers: A strategy to offset the energy cost of CCS" [2].

CMG's compositional numerical reservoir simulator GEM was used to obtain the results of their study. GEM is good for modelling fluid- and geological complexities of such processes. They also used GEM's wellbore model to help calculate bottomhole pressures and fluid rates associated with wellhead pressures. Finally, the Peng-Robinson equation-of-state [12] was used to model their fluids.

Some of the points of interests for the simulation were the injection flow rates of carbonated brine versus the production flow rates of methane brine. The injection rate was kept constant for all the different cases. The production rate of methane however, increased with increasing depth – an indication of the pressure effect on methane solubility in brine.
The rate of produced brine also increased with depth. Although it is not stated in the study, one could assume this increase is due to methane brine compressibility versus carbonated brine compressibility. If we look at the ideal gas law, and take into consideration the compressibility of a real gas, it takes on the form:

$$PV = ZnRT \qquad (3.1)$$

In equation (2.11), R is the universal gas constant and n is the number of moles of gas. A mole has a value of $6.022\ 140\ 857 * 10^{23}$. Without going into too much detail, the high value of the mole unit has to do with the number of atoms there are in 12 grams of carbon-12 [13]. Because atoms are so small, the high value of a mole is convenient when doing calculations and measurements on a macroscopic scale. Carbon-12 is an isotope of carbon. Each element, including carbon, has a certain number of protons and neutrons making up its atomic nucleus. Carbon atoms can have different isotopes, all contain the same number of protons, but differ in number of neutrons [14].
The compressibility factor, Z, in this equation says something about the change in volume of said fluid when being subject to pressure. Ideal gasses have a Z-value of 1 [15]. T is the absolute temperature of the gas – measured in Kelvin if SI-units are employed. Zero degrees kelvin is equal to -273.15°C, where particles have minimum motion, or zero kinetic energy [16].

V denotes the volume of the gas and P denotes the pressure of the system. However, we can substitute the volume with:

$$V = \frac{m}{\rho} \qquad (3.2)$$

In equation (2.12), m is the mass of the gas and ρ is the density of the gas. Because different gases vary in density - if you have systems subject to the same pressure, same mass of respective gases, same number of moles and being at the same temperature – the gases would have different compressibilities according to this gas equation. For this reason, one could assume different gases dissolved in liquids could adopt different compressibilities as reflected in the study of Ganjdanesh and his team.

In their simulation, the injection rate of carbonated brine was set to '38 300 STB/Day' for all nine depths. STB is short for stock tank barrel and is a measure of volume used in the petroleum industry. The production rate of methane brine increases after the depth of 11 000ft. At the deepest, 16 000ft, the production rate of brine was '41 900 STB/Day'.

Part of this study's objective was to do an energy analysis and to compare the energy consumption of a 500MW power plant, if it were set to do a CCS operation, to the energy the power plant could generate from the same aquifer. The study looked at the power consumption of each step of the CCS process independently. As mentioned earlier, the capture and pressurization steps consume the most energy. To calculate the energy required to pressurize the CO_2 to mixing condition, they used the polytropic equation [(A.1) in Appendix]. To calculate the energy required to pressurize the brine to mixing condition, they used the equation of mechanical energy balance [(A.3) in Appendix]. The heat extracted from the produced brine, they assumed, was to be used in an organic Rankine cycle (ORC). The thermal efficiency of the ORC was found using a correlation obtained from data of existing ORC geothermal power plants [(A.4) in Appendix].

An ORC can produce power from heat sources that have temperatures ranging between 80°C and 350°C. The ORC uses organic fluids in its cycle. The organic fluids have lower boiling points and higher vapor pressures than water. These properties make the organic fluid able to extract energy from, relatively, low-temperature sources, i.e. ones that have temperatures between 80°C and 350°C. The heat source interacts with a heat exchanger. The exchanger heats an intermediate fluid which transfers heat to the organic fluid. The vapor of the organic fluid powers turbines, which in turn produce electricity. The vapor is then condensed back into a liquid before it is pumped back to where it will be reheated by the intermediate fluid, completing the cycle [17].

The methane, was assumed, could be used in a gas cycle power plant or gas engine. The gas engines use the heat from combusted methane to produce usable energy. The efficiency of methane combustion can reach 47%. The pressure gradient and temperature gradient increase more rapidly after a depth of 10 000ft. This zone is what is known as a geopressured-geothermal formation. The increase of the pressure gradient is mostly due to compaction. Compaction happens when rock gets compressed due to high pressures. The fluid that gets exposed to these high pressures, generates a higher than normal porosity in the rock and also has a low thermal conductivity. The conductivity says something about a fluid's ability, or material's ability, to transfer heat to another fluid or material. If the thermal conductivity of the fluid is low, then the fluid has a good ability to retain heat. This is the reason why the geothermal fluid can stay hot over time and not lose too much heat to the surrounding formation.

The study found that production of geothermally-heated methane brine from depths below 11 000ft, equalized their power plant's energy consumption of using CCS [2].
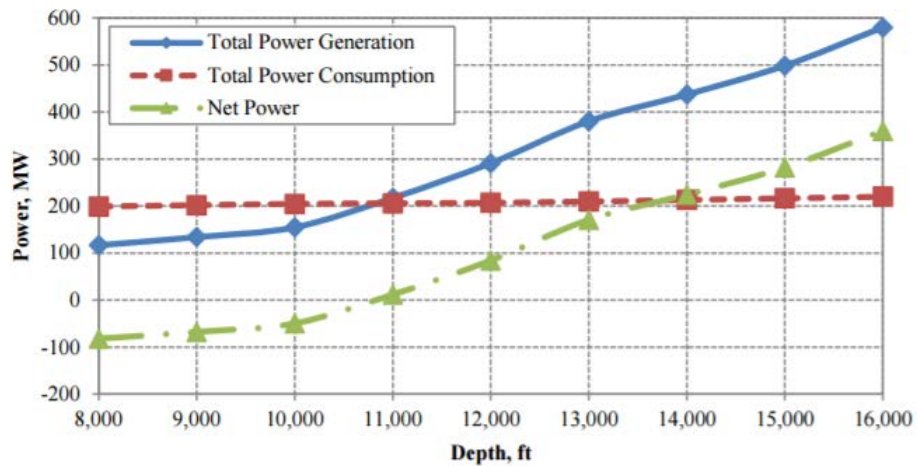

Figure 3.2: Showing at which depth the power generation offsets the power consumption – at 11 000ft, the net power is zero [2].

3.2   Dissolved CO_2

To really solidify the choice of using carbonated brine as a displacing fluid in deep saline aquifers, comparing the results of the previous study with one that used supercritical CO_2 to displace aquifer fluid should be examined. In 2014, Reza Ganjadanesh et. al. presented an SPE paper titled: "Coupled Carbon Dioxide Sequestration and Energy Production from Geopressured/Geothermal Aquifers" [3]. In the paper, Ganjdanesh again looks at the benefits of using CO_2 dissolved in brine as an injection fluid. But additionally, a comparison is made with supercritical CO_2 as the injection fluid. Mole fractions at breakthrough time of both cases are modelled, as well as other interesting energy production essentials.

One of the points mentioned in this paper, as opposed to the previously discussed paper, is that the carbonated brine that is to be injected, would make use of waste brine. In other words, instead of using a separate brine for injection, one would re-inject the produced brine after it has served its purpose. This tactic would save money in more than one way. Re-injection would eliminate the problem of having to dispose of tonnes of leftover brine. Additionally, this method removes the need to get ahold of the brine required for injection in the first place. The inadequacies of injecting supercritical CO_2 are also stated in the paper. For example, the pressure buildup constraining the amount of CO_2 that can be sequestered is mentioned.

When using supercritical CO_2 as an injection fluid, the CO_2 will mix with the brine in the aquifer. When this happens, the methane will escape the brine and flow upwards. If a production well is placed higher in the aquifer, it can collect the methane. The depth placement of the injection well versus the production well is therefore opposite compared to the case where carbonated brine used.

To model the fluids to be used in the simulation, the Peng-Robinson equation-of-state [12] was used. Field data from the Gulf of Mexico were again used for their aquifer parameters. Calculations regarding

14

solubility needed for the simulation were done using CMG WinProp PVT Software. In the subchapter 'Carbonated Brine and Chemistry' of my thesis, CO_2 solubility in brine was discussed. In Ganjdanesh's paper, they modelled the molar solubility ratio of carbonated brine to methane brine and found that it was approximately 6:1 in the geopressured geothermal zone. The molar solubility basically says something about how concentrated a solution is – how many moles of a substance there are per unit volume, usually measured in liters, before the solution becomes saturated [18].

After having developed the aquifer model for the simulation, two different injection strategies were investigated. One method would be to inject supercritical CO_2 and produce methane gas and brine with dissolved methane. The second method would be to inject brine with dissolved CO_2 and produce brine with dissolved methane. Another benefit of using carbonated brine, is that most of the methane gas can be removed from the produced brine at the surface without having to reduce the pressure too much. The reason for the insignificant pressure reduction is not directly stated in the paper. However, one might assume that what Ganjdanesh referring to, is that when supercritical CO_2 is used as an injection fluid, methane escapes the brine inside the aquifer. This results in a gas production. When using carbonated brine as an injection fluid, there is no interchanging of gases with the residual brine – CO_2 remains in the injected brine and methane remains in the produced brine. The small pressure reduction also, one could assume, states that a larger pressure reduction is not necessarily needed to extract most of the methane from the produced brine. If active surface handling of fluids is minimal, the process in itself will be cheaper.

For the simulation, both vertical wells and horizontal wells were used as injection and production wells. There are different aquifer, or reservoir, parameters that affect the efficacy of the different well types. The aquifer parameters considered in the paper were: "vertical permeability, horizontal permeability, porosity, relative permeability, capillary pressure, depth, thickness, temperature, pressure, brine salinity, PV, and methane concentration in brine.", where 'PV' is referring to the pore volume. The importance of PV escapes me as porosity is already being considered. Porosity is the ratio of pore volume of the aquifer to the total volume of the aquifer. The remaining parts of the aquifer, the matrix, are not relevant for storing capacity.

Permeability is a porous medium's ability to have a fluid flow within it in interconnecting channels. To displace the fluid that is initially in the aquifer, or reservoir, and be able to inject any fluid into the aquifer in the first place, the aquifer needs to be permeable. As mentioned earlier in my thesis, if a formation is permeable all the way to the seafloor, the pore pressure in the formation is equal to that pressure which a column of seawater would generate to that same depth. A reservoir needs to have horizontal permeability as well as vertical permeability. The horizontal permeability, intuitively enough, affects the breakthrough time of CO_2. Permeability's SI-unit is meters squared (m^2), but it is most commonly measured in 'darcy' or millidarcy for practical purposes (1 darcy $\approx 10^{-12} m^2$) [19].

Capillary pressure is a factor that needs to be considered regarding flow initiation. If there are two different fluid phases in a pore, there exists an interfacial tension between the two phases. This tension needs to be exceeded by the entering fluid for flow to take place inside the aquifer [20].

Flow of more than one phase in a permeable formation is were relative permeability comes into play. It is a ratio of one phase's effective permeability to the absolute permeability. The effective permeability is the permeability of said phase and the absolute permeability makes up the sum of all the phases' permeabilities. However, because the presence of other phases usually inhibit the flow of another phase, the sum over all relative permeabilities become less than 1 [21]. In the case of injecting a fluid into an aquifer, this phenomenon of relative permeability becomes relevant when supercritical CO_2 is used. Because the supercritical fluid is a mix between a gas and a liquid, there is more than one phase present. Additionally, when the supercritical fluid is used, methane is released from the methane brine.

In the paper, when carbonated brine was simulated as the injection fluid, reservoir pressure was kept above that of the injected brine. This would ensure an aqueous liquid only, cancelling the need for relative permeability to be taken into account [3].

The relative permeability can be expressed as a function of water saturation – how much water are in the pores. If certain approximations are used in the relative permeability equations, 'Corey' correlations may be implemented. These correlations are power laws, which in this case means that the value of the relative permeability varies as a power of Corey's empirically derived constants [3]. In the simulation, initially one correlation for the gas's relative permeability could be used and another for the water's relative permeability [(A.5) and (A.6) in Appendix].

However, when modelling flow in an aquifer, or reservoir, the effect of 'hysteresis' plays a part. There is a wetting phase and a non-wetting phase inside the reservoir. The wetting fluid phase is the phase that spreads out on the rock, or inside on the pore walls. The non-wetting phase is therefore not in contact with the pore wall. For this reason, the relative permeability of a fluid acts differently under reservoir drainage than under reservoir imbibition. Under reservoir drainage, the wetting phase saturation decreases. This would be the case if one uses non-wetting fluid to displace a wetting fluid. Under reservoir imbibition, the wetting phase saturation increases. This would be the case if one uses a wetting fluid to displace a non-wetting fluid. In other words, the history of the reservoir has an effect on the displacements happening, relative permeabilities and capillary pressures. For instance, capillary pressures can be plotted against water saturations on hysteresis plots. On these plots, a significant difference can be seen on the imbibition curve versus the drainage curve regarding capillary pressures. The capillary pressure depends on the water saturation and on the direction of the saturation, whether an imbibition or drainage is taking place in the reservoir [3] [20], [21].

In the simulation, hysteresis was taken into account. The reason for including hysteresis in their model, was that trapped-gas saturation has a significant effect on CO_2-sequestration. The Corey correlations must be modified to incorporate the effect of hysteresis. The simulator used for the study uses a modified 'Land' equation for this purpose [3], [(A.7), (A.8) and (A.9) in Appendix].

In addition to modelling and studying homogeneous-aquifer cases, heterogeneous-aquifer cases were also modelled and studied. Homogeneity describes something, e.g. a formation, which is uniform in structure. A reservoir that does not differ in characteristics depending on where you take a measurement from, can be classified as a homogeneous reservoir. A heterogeneous reservoir's characteristics would differ throughout its volume. The latter case is, of course, the more realistic approach to take when studying a formation. Due to all the complexities that follows with heterogeneity, approximations have to be made so that sections of a reservoir can be considered homogeneous. However, if one account for certain changes throughout a reservoir, e.g. a reservoir that consists of more than one layer and each layer has different characteristics, then that reservoir can be considered as a heterogeneous one. In the simulation, layered sequencing was used to study the effect of heterogeneity on storage and production [3].

Finally, to figure out the energy consumption of the process as a whole, there needs to be a connection between the well injection point and well production point to the surface where the pumps and processing units are located. CMG's compositional simulator GEM was used to combine a wellbore model with the aquifer. The wellbore model incorporates hydrostatic pressure with different types of pressure drops that happen in drilling operations. There is a pressure drop caused by kinetic energy and by friction when there is fluid flow. For the injection fluid to enter the aquifer, a certain amount of pressure needs to be put on the injection fluid to equalize the pore pressure of the aquifer. The hydrostatic pressure, due to the weight of the column of fluid in your wellbore, will work in your favor.

The pressure drops caused by friction and by kinetic energy will work against you. Adding up the three pressure differentials will give you some idea of the pressure required to be put on the injection fluid at the surface. However, there is also the matter of pressure drop along the length of the aquifer [3].

When pumping a fluid over a length, the pressure of the fluid at the end point versus the beginning will not be the same. Pressure drops cause a decrease in fluid pressure at the end point. Friction resists the fluid's motion and therefore acts against it, causing a pressure drop. The friction factor will depend on what type of fluid is being used. Fluid types can be described as Newtonian or non-Newtonian fluids. Each fluid type has a certain viscosity – a resistance to deformation when being subjected shear stress. If picturing a fluid flowing in a pipe, one can imagine the fluid consisting of a number of thinner layers flowing parallel to each other. If the layers closer to the center of the pipe flow faster than the decentralized layers, a shear stress will act on the surface between the layers. The shear stress if proportional to the viscosity if a Newtonian fluid is being considered. However, when non-Newtonian fluids are used, which is usually the case for drilling fluids, the viscosity is a function of shear stress and is not proportional. The friction factor will also depend on the Reynolds number. The Reynolds number gives an indication whether the fluid flow is laminar or turbulent. A fluid flow is laminar when the layers in the fluid flow parallel to each other. If the relative roughness of a pipe wall is high, there is a bigger chance of the flow being turbulent. When the flow is turbulent, the fluid layers behave more chaotically, intersect and are indistinguishable from one another. In the case of turbulent flow, empirical models are used to describe a flow's characteristics due to the complexity [22]. In the paper of Ganjdanesh, laminar flow is assumed in the injection well. As for whether a Newtonian or non-Newtonian fluid is assumed, brines are usually classified as Newtonian fluids [22]. Although, the brine being injected is saturated with CO_2 gas.

In the paper, the pressure loss associated with kinetic energy, I believe, has to do with conservation of energy. Bernoulli's principle describes energy conservation in fluid dynamics. Bernoulli's equation is the sum of a fluid's hydraulic head, the fluid's dynamic pressure and the fluid's pressure. The hydraulic head constitutes the system's elevation from point A to point B. The dynamic pressure constitutes the fluid's speed. If there is an increase in fluid speed, the fluid pressure must decrease for the system's energy to be conserved. However, this is the case for incompressible fluids. Other assumptions must also be put on the fluid system: the flow must be steady, friction by viscous forces has to be negligible and the measurements have to be taken along a streamline. Steady flow means that the velocity at a certain point in the fluid does not change with time. For the measurements to be taken along a streamline, one must assume a laminar flow. There exist relatively more complex equations for flow of compressible fluids [23]. Which assumptions have been made regarding fluid compressibility have not been stated in the paper.

3.2.1 Results

Before going into the results of the paper, a few more factors regarding their simulations should be mentioned. The dimensions of the aquifer, for the homogeneous case, was set to 10 560*10 560*300 feet. In metric units, that volume would equal approximately 3 218*3 218*91 meters. A horizontal injection- and horizontal production well was used. The wells were positioned along the 10 560 feet lengths of the aquifer. The injector was placed low in the aquifer, and the producer high, to displace the methane-brine upwards. This tactic made the displacement gravitationally stable, ensuring a higher sweep efficiency.

The bottomhole pressure was kept constant. Meaning, during a simulation run, the injection pressure and production pressure does not vary with time. The initial mole fractions for the methane-brine were set to 0, 0.0037947 and 0.9962053 for CO_2, methane and water, respectively. The mole fractions of the carbonated brine were 0.0221352 and 0.9778648 for CO_2 and water, respectively. The injection and production periods were determined by the CO_2-breakthrough time.

The comparison of the two injection strategies proposed is intriguing. For the method of using dissolved CO_2, approximately 27.4 billion cubic feet of methane was produced. That approximation is measured at surface conditions were the pressure is lower than in the aquifer. From this amount of methane, heat corresponding to 28.2 trillion Btu can be generated. Btu (British thermal unit) is a unit used for measuring heat and is the required heat to raise the temperature of one pound of water by one degree Fahrenheit [24]. The produced brine amounted to 810 STB at 300°F. The energy that can be extracted and exploited by reducing the temperature of the produced brine from 300°F to 200°F is approximately 28.3 trillion Btu.

For the method of using supercritical CO_2, approximately 15.5 billion cubic feet of methane was produced. From this amount of methane, heat corresponding to 15.9 trillion Btu can be generated. Approximately 457 million STB of brine was produced, also at 300°F. Making use of the same temperature reduction, 16.0 trillion Btu can be extracted [3].

The first strategy, using carbonated brine, injected fluid over a period of 8 337 days, or 23 years. The second strategy, using supercritical CO_2, injected fluid over a period of 4 449 days, or 12 years. This contrast in injection periods has to do with CO_2-breakthrough time. For the carbonated brine, approximately 8.3 million tonnes of CO_2 was injected. Compared to the supercritical CO_2, 70.0 million tonnes of CO_2 was injected. For supercritical CO_2, more than eight times the volume of CO_2 can be injected over half the time interval. However, using supercritical CO_2 requires getting rid of a very large volume of waste brine. Another disadvantage of using supercritical CO_2 is that its low density, compared to carbonated brine, requires more pumping at the surface to meet the bottomhole pressure, meaning higher pumping costs [3].
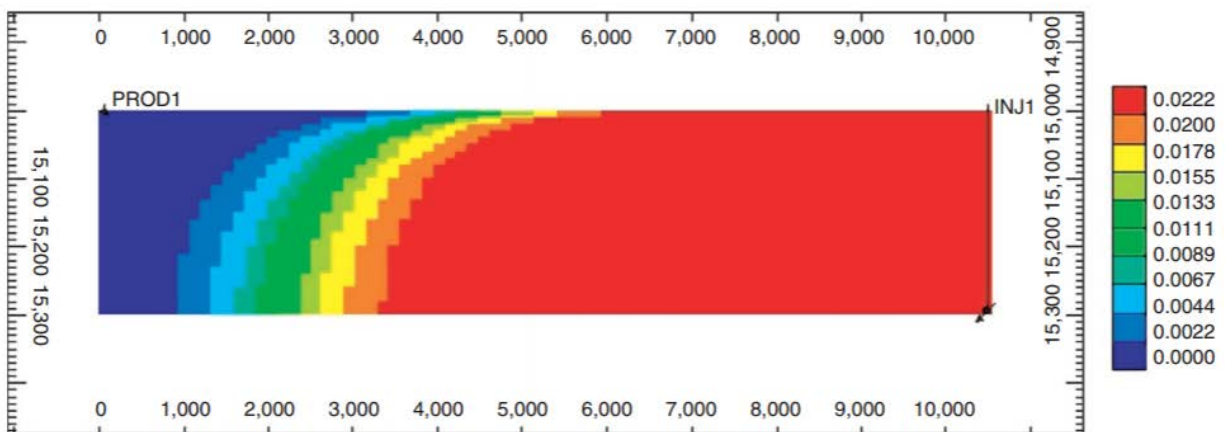

Figure 3.3: Mole fraction of CO2 at CO2-breakthrough time when using carbonated brine [3].
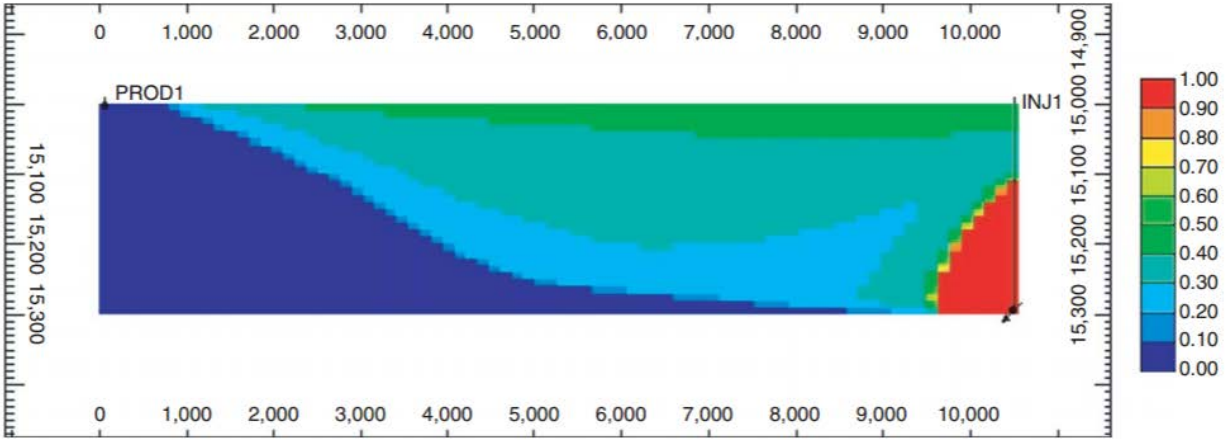
Figure 3.4: Mole fraction of CO2 at CO2-breakthroughtime when using supercritical CO2 [3].

As can be seen on the figures above, the CO_2-front on figure 3.3 is much sharper, and the sweep efficiency much higher, than that of figure 7. The reason for this difference is threefold. One, the mobility ratio in the first scenario is much lower – brine is displacing brine. Two, when a denser brine is displacing a less dense brine, the displacing process is gravitationally stable. Three, when using carbonated brine, there is less mixing between CO_2 and methane in the aquifer. At a first glance, there might seem to be stored more CO_2 for the case of using carbonated brine when looking at the figures. But, the mole fractions on figure 3.4 are much higher than those represented in figure 3.3 [3].

3.2.2   More findings for dissolved CO_2 injection

Eight cases were simulated with dissolved CO_2 as injection fluid in the case of a homogeneous aquifer. Different well spacings were used for each case. Case one through three utilized a horizontal well pattern. Case four through eight utilized a vertical five-spot well pattern. The recovery rates of methane and brine were basically the same, independent of aquifer size. However, it was found that recovery rates would be almost 20% higher when using horizontal well patterns compared to the vertical well patterns.

The effect of permeability on storage and production on vertical wells was also studied. They simulated six cases with varying horizontal- and vertical permeabilities. The ratio between the two permeabilities was kept the same for all six cases. The case with the highest horizontal permeability had the earliest CO_2-breakthrough time. The energy recovery for all six cases was essentially equal [3].

Finally, the effect of heterogeneity on storage and production was studied. Three rock types with varying parameters were randomly assigned to the aquifers 30 layers. The aquifer model volume was set to 5 280*5 280*300 feet. Each rock layer would then be 10 feet. The energy recovered when implementing horizontal wells was more than twice the amount of that which could be recovered using vertical wells. One of the reasons for the lower energy recovery when using vertical wells, is that there is an earlier CO_2-breakthrough. When using horizontal wells and the permeability is low, the vertical migration of fluids is limited and breakthrough happens later [3].

19

3.2.3 More findings for supercritical CO_2

The same strategies were employed to figure out the benefits and limitations of different variables when using supercritical CO_2 as an injection fluid. Eight cases with varying aquifer dimensions were used to study the effect of well spacing and well types on storage and production. Case 1 through 3 used horizontal wells. The most significant finding was the amount of CO_2 that could be stored in a relatively short time period. Case 4 through 8 used vertical wells. Here, case 4 showed most promising given its dimensions. Albeit, the volume of the aquifer in case 4 was bigger than the volumes for case 5 through 8, it showed better results proportionally. The length and width of case 4 was 5 280*5 280 feet. The aquifer thickness was kept at a constant 300 feet for all eight cases. Permeability was also kept constant for all eight cases [3].

Permeability ratios were investigated on six simulations. 0.01, 0.02, 0.05, 0.1, 0.5 and 1 were used, where the ratios signal vertical permeability over horizontal permeability, or $\frac{k_v}{k_h}$. It was found that a higher vertical permeability caused an earlier CO_2-breakthrough. The earlier breakthrough caused a lower storage and production output.
The same setup used for dissolved CO_2 was used to study effect of heterogeneity on storage and production when using supercritical CO_2. It was discovered that 60% more energy could be produced if horizontal wells are used compared to vertical wells.
The impact of hysteresis was also investigated with varying trapped-gas saturations. Saturations ranging from 0.0 to 0.3, with incremental steps of 0.1, were tested. In the case of homogeneous aquifers, hysteresis seemed to have no impact. In the case of heterogeneous aquifers, hysteresis had no effect on vertical wells, however, hysteresis did affect the horizontal wells. If the trapped-gas saturations are high, and certain layers have low permeability, the trapped gas will prevent the CO_2 from flowing upwards. The lower density gas will act as a barrier, trapping the CO_2. The trapped gas will therefore significantly hinder the CO_2 injectivity potential [3].

3.2.4 Conclusions

An important conclusion made in the paper about the method of dissolved CO_2 injection, is that five times more CO_2 can be stored than what would be produced when burning the produced methane. The same method therefore offers a great way to offset the costs of carbon capture and storage [3]. As discussed earlier in my thesis, there are possibilities of CO_2 leakage when using supercritical CO_2 as an injection fluid. On the contrary, the stability of CO_2 stored underground was also discussed. Because there are interactions between the CO_2 and the in-situ brine, and furthermore the aquifer minerals, balanced and stable relationships may be established. The example mentioned in my thesis, suggested CO_2 that had been stored underground for approximately 70 million years. Additionally, a larger volume of CO_2 may be injected when using supercritical CO_2.
The dissolved CO_2 injection method by comparison, has increased reliability due to physical similarities with the aquifer brine. It shows greater energy recovery rates. For dissolved CO_2, produced brine may be reused and excess brine, therefore, need not be discarded [3].

TABLE 12—PRODUCED AND CONSUMED ENERGY PER TONNE OF STORED CO_2			
Injection Strategy	Total Produced Energy (kW·h)	Energy for Compressing CO_2 (kW·h)	Energy for Pumping Brine (kW·h)
Dissolved CO_2	2,000	105	240
SC CO_2	135	110	0

Figure 3.5: Table from "Coupled Carbon Dioxide Sequestration and Energy Production from Geopressured/Geothermal Aquifers" [3].

4 Simulation

In this part of the thesis, a more detailed description of what is to be done using the simulator will be explained. The simulator that was chosen for this thesis was CMG STARS. The simulator is able to model advanced processes that take place in a reservoir. It is also a thermal reservoir simulator, making it a useful tool in modelling geothermal and geopressured reservoirs. The STARS User Guide – version 2016 gives an insight into the equations that govern the relatively complex physical phenomena that take place in a reservoir. Before looking at which models the simulator can produce, it would make sense to review some of the equations making the models possible.

4.1   In the reservoir

For physical systems to work, there needs to be a conservation of energy, or mass. The same condition applies to the CMG STARS simulator. The simulator phrases the conservation principle as:

$$
\begin{aligned}
&\quad\text{rate of change of accumulation}\\
=\;&\quad\text{net rate of inflow from adjacent regions}\\
+\;&\quad\text{net rate of addition from sources and sinks}
\end{aligned}
\tag{4.1} \quad [25]
$$

In the simulator, grids are used to represent a reservoir model. This means the reservoir is made up of blocks, or cells, of a certain size determined by the user. The grid blocks contain different volumes of interest. At the start of the simulator run, the following volumes are being considered:

V_b	Current bulk volume
V_b^0	Initial bulk volume
V_r	Rock volume (solid matrix, rock grains)
V_v	Void volume (fluids and variable solids)
V_s	Volume of solid, adsorbed and trapped components
V_f	Volume of fluid phases added together
V_w	Volume of water (aqueous) phase
V_o	Volume of oil (oleic) phase
V_g	Volume of gas (vapor) phase

The bulk volume refers to the volume of the whole reservoir and is the sum of the rock volume and the void volume.

$$V_b = V_r + V_v \tag{4.2} \quad [25]$$

The void volume refers to porosity and is the volume of the reservoir occupied by pores. The current fluid volume is a sum of all fluids in the reservoir:

$$V_f = V_w + V_o + V_g \tag{4.3} \quad [25]$$

The w, o, g indices denote water, oil, and gas, respectively.
The void volume can be derived from equation (3.2):

$$V_v = V_b - V_r = V_f + V_s \qquad\qquad (4.4) \quad [25]$$

The void porosity is a dimensionless ratio and can be defined as:

$$\varphi_v = \frac{V_v}{V_b^0} \qquad\qquad (4.5) \quad [25]$$

As a reservoir is under production, there may occur changes to the bulk volume, or equation (3.2). For this reason, it is commonplace to measure a *true* porosity, using the current bulk volume. Equation (3.5) therefore represents the *reservoir* porosity with initial bulk volume. However, the STARS simulator uses reservoir porosity with a few exceptions.

By the same thinking, one can define a current fluid porosity combined with equation (3.4):

$$\varphi_f = \frac{V_f}{V_b^0} = \frac{V_v - V_s}{V_b^0} = \left(\frac{V_v}{V_b^0}\right)\left(1 - \frac{V_s}{V_v}\right) = \varphi_v\left(1 - \frac{V_s}{V_v}\right) \qquad\qquad (4.6) \quad [25]$$

From equation (3.6), the term $\frac{V_s}{V_v}$ appears. This term makes up the fraction of the void volume occupied by the solid/trapped/adsorbed component. Adsorption is a surface phenomenon, and happens when a fluid or dissolved solid adheres to a surface, making a film [26]. The abovementioned fraction may be written as:

$$\frac{V_s}{V_v} = \sum \frac{c_{si}}{\rho_{si}} \qquad\qquad (4.7)$$

Here, c_{si} is the molar concentration of component i in the void volume. ρ_{si} is the molar density of pure component i in the void volume. The molar concentration is the number of moles of a component per liter. The molar density is the number of moles of a component per unit of volume. Inserting equation (3.7) into (3.6) yields:

$$\varphi_f = \varphi_v\left(1 - \sum \frac{c_{si}}{\rho_{si}}\right) \qquad\qquad (4.8) \quad [25]$$

From equation (3.8), one can see that the fluid porosity would be equal to the void porosity if there are no solid, trapped or adsorbed components.

The different saturations regarding the reservoir's properties are defined as following:

$$S_w = \frac{V_w}{V_f}$$

$$S_o = \frac{V_o}{V_f}$$

$$S_g = \frac{V_g}{V_f}$$

$$S_w + S_o + S_g = 1 \qquad\qquad (4.9) \quad [25]$$

These saturations are usually affiliated with hydrocarbon-reservoirs. In the simulation for this thesis, deep saline aquifers are being considered. Although an aquifer contains different fluids than an oil reservoir does, similar saturation relations would pertain. As mentioned in chapter 2, when reviewing

"Coupled Carbon Dioxide Sequestration and Energy Production From Geopressured/Geothermal Aquifers", aquifers may contain trapped gas. Also, sweep efficiencies do not reach 100%, making the aquifers consist of different fluids, or different saturations.

Looking at equation (3.1), the first term represents accumulation in the mass conservation principle. The STARS guide lists three accumulation terms. The first term is for flowing and adsorbed components. The second term is for solid components. The third term is for accumulation of energy.

$$\frac{\partial}{\partial t}\left[V_f\left(\rho_w S_w w_i + \rho_o S_o y_i + \rho_g S_g x_i\right) + V_v A d_i\right] \qquad \text{(4.10)} \quad \text{[25]}$$

$$\frac{\partial}{\partial t}\left[V_v c_i\right] \qquad \text{(4.11)} \quad \text{[25]}$$

$$\frac{\partial}{\partial t}\left[V_f\left(\rho_w S_w U_w + \rho_o S_o U_o + \rho_g S_g U_g\right) + V_v c_s U_s + V_r U_r\right] \qquad \text{(4.12)} \quad \text{[25]}$$

The partial derivative taken on each term represents a change in accumulation over time. When partial derivatives are taken, the derivative is taken with respect to one variable in the function, or in this case term, and the other variables are held constant. In (3.10), mass flow of the different phases are taken into account. The first part of (3.10) takes the volume of the fluid phases added together, V_f, and multiplies it with the densities of the respective phases. The saturations of the respective phases weighs the volume of each phase to the fraction of volume the different phases occupy. w_i, y_i, x_i and d_i represent the different flow rates of the respective phases. The last term in (3.10) is the amount of adsorbed components, and their flow rate.
c_i in (3.11) is the concentration of solid components. Because this equation represents solid components, there is no flow rate involved.

In (3.12), U represents the different phases' internal energies as a function of temperature and phase composition. c_s is the total concentration of all the solid components added together. The ρ in (3.10) and (3.12) are the phase densities.

The second term in equation (3.1) takes into consideration the flow between two regions:

$$\rho_w v_w w_i + \rho_o v_o x_i + \rho_g v_g y_i + \phi \rho_w D_{wi} \Delta w_i + \phi \rho_o D_{oi} \Delta x_i + \phi \rho_g D_{gi} \Delta y_i \qquad \text{(4.13)} \quad \text{[25]}$$

In (3.13), the volumetric flow rates of the different phases are represented by the small letter v, each phase with its own index. In the simulator, the volumetric flow rate is defined as:

$$v_j = T\left(\frac{k_{rj}}{\mu_j r_j}\right)\Delta \Phi_j \qquad \text{(4.14)} \quad \text{[25]}$$

j represents the different phases. T denotes the transmissibility between two regions. The transmissibility takes into account cross sectional area, the length between the two points where flow is happening and the permeability at the interfaces between said regions. k_{rj} is the effective permeability, μ_j is the viscosity of the phase. Viscosity is a measure of a fluids resistance to deformation – a highly viscous fluid shows greater resistance to flow than a less viscous fluid. r_j is a resistance factor. The factor

will normally be set to 1.0, but large values of r_j can be seen as blocking phenomena. The aquifer, or reservoir, model built in CMG STARS will consist of many points, or nodes, in each grid block. $\Delta \Phi_j$ denotes a pressure difference, or potential, between two nodes.

The D_{ji} for the different phases in (3.13) represents dispersion. Dispersion can happen when there is a heterogeneity of permeability in the reservoir. The fluids in the reservoir may then take different paths and a separation of components within a fluid takes place [27]. w_i, x_i, y_i make up the fractions of each phase. It is not stated directly in the STARS guide, but I believe $\Delta w_i, \Delta x_i, \Delta y_i$ make up the amount of the phases' fractions not dispersed. ϕ may represent the next node, but is also not directly explained in the guide.

There is no flow of solid components, which means no equation explaining it is warranted. The flow of energy, however, is defined as:

$$\rho_w v_w H_w + \rho_o v_o H_o + \rho_g v_g H_g + K\Delta T \qquad (4.15) \quad [25]$$

In (3.15), H_j of the different phases, represents energy in the thermodynamic system. K is the thermal transmissibility. The thermal transmissibility shares the same principles as T in equation (3.14), only the K has to do with thermal conductivity. The ΔT from (3.15) is the difference in temperature from one node to the next. If $\Delta \Phi_j$ or ΔT is negative, it means outflow. If the same terms are positive, they represent inflow.

Looking at equation (3.1) again, the last expression makes up for so-called source and sink terms. When depleting, or producing from, an oil field, it is common practice to use an injection well to help boost the oil recovery. Seawater, among other concoctions, can help displace the oil or gas present in the reservoir. The injection of fluids help maintain reservoir pressure. The fluids used are also denser than the oil and gas, displacing the oil and gas upwards. The process of injection to increase production is known as 'EOR', or enhanced oil recovery. As explained earlier in this thesis, the same thinking applies when displacing methane-filled brine with carbonated brine. Only in the latter case, the goal is also to store CO_2. However, different methods of CO_2 injection exist in EOR as well.
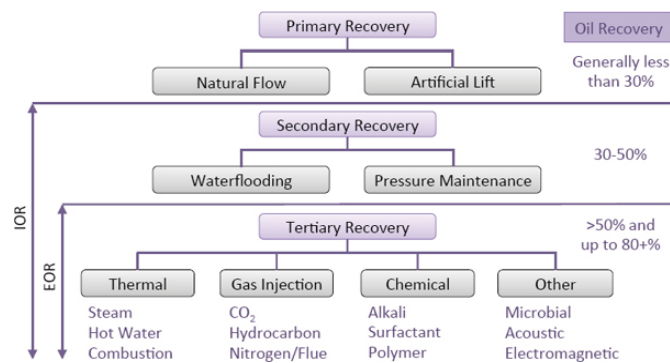

Figure 4.1: Showing the definition nuances between IOR and EOR [28]

In figure 4.1, different EOR methods are listed. The figure also introduces 'IOR', or increased oil recovery. The figure also details which recovery rates can be expected by using the different methods of injection.

IOR encompasses EOR, but EOR is prescribed to the recovery rates exceeding 50%.
The source/sink term for flowing component i is:

$$\rho_w q_{wk} w_i + \rho_o q_{ok} x_i + \rho_g q_{gk} y_i \qquad \text{(4.16)} \quad [25]$$

The source/sink term for energy is:

$$\rho_w q_{wk} H_w + \rho_o q_{ok} H_o + \rho_g q_{gk} H_g \qquad \text{(4.17)} \quad [25]$$

As when considering flow between two regions, the solid components have no terms in regards to source/sink. (3.16) and (3.17) look eerily similar to (3.13) and (3.15). In fact, the volumetric flow rate here, q_{jk}, is comparable to v_j, but is calculated differently:

$$q_{jk} = I_{jk}(p_{wfk} - p_k) \qquad \text{(4.18)} \quad [25]$$

Because the well, injection or production, most likely will be completed through more than one zone, or layer, the k refers to the layer of interest. I_{jk} specifies the phase j index for well layer k. p_k denotes the node pressure at the point of interest which contains layer k. Finally, the p_{wfk} denotes the flowing wellbore pressure in the same layer k.
When p_{wfk} is higher than p_k, q_{jk} will be positive. A positive q_{jk} indicates an injection setting and fluid properties will be taken from wellbore conditions. When p_{wfk} is lower than p_k, q_{jk} will be negative. A negative q_{jk} indicates a production setting and fluid properties will be taken from the producing region.

Similarly to (3.16) and (3.17), there exists terms describing the same source/sink relations for thermal aquifers:

$$\sum_{k=1}^{n_f} \rho_w q a q_{wk} \qquad \text{(4.19)} \quad [25]$$

$$\sum_{k=1}^{n_f} (HA_{CV} + HA_{CD})_k \qquad \text{(4.20)} \quad [25]$$

In term (3.19), $q a q_{wk}$ describes the volumetric flow rate of water through a block face in your grid to or from the adjacent aquifer. n_f is the number of neighboring regions to the block of interest where the is an interaction. In term (3.20), HA_{CV} is the heat transferred by the adjacent aquifer by convection. The heat transferred by conduction from or to the adjacent aquifer is represented by HA_{CD}. Convection is the phenomenon that happens due to density discrepancies in a heated fluid. The warmer part of a fluid rises due to its lower density. The warmer fluid displaces the colder fluid, making the colder, denser, fluid sink. If one imagines a cooking pot, the warm water would rise in the middle, then cool off and sink along the edges of the pot. The reason the water is more prone to rise in the middle compared to the edges, has to do with the middle being less exposed to the colder environment. The convection phenomena happens in the earth's mantle, below the crust, as well. In the earth's mantle, a continuous stream of hot magma heats the earth's crust by convection, and ultimately conduction. The continuous heat supply from the mantle gives the earth's crust a geothermal gradient, which in turn allow for geothermal/geopressured reservoirs to form. Convection may happen on small and large scales - the earth's mantle would represent a huge scale, and the convection happening inside a reservoir due to the adjacent heated formation would be on a much smaller scale.

The simulator also takes into consideration chemical reactions and interphase mass transfer source/sink terms. The reason for this has to do with the fact that the injection fluid, most likely, will not be the same, chemically, as the fluid it is displacing. For component i, the reaction source/sink term is defined as:

$$V \sum_{k=1}^{n_r} (s'_{ki} - s_{ki}) r_k \qquad (4.21) \quad [25]$$

For energy, the source/sink term is defined as:

$$V \sum_{k=1}^{n_r} H_{rk} r_k \qquad (4.22) \quad [25]$$

In expression (3.21), the V is volumetric flow rate. n_r, although it is not directly stated in the guide, most likely refers to the number of neighboring regions where there is a reaction interface. s'_{ki} is the product stoichiometric coefficient of component i in reaction k. Stoichiometry refers to a chemical reaction where the quantities of the different chemicals reacting is taken into account. If one is looking at the product of a chemical reaction, one can calculate the quantities of the chemicals that have been put in to react. Vice versa, one can calculate the quantities of the product, knowing the reactants [29]. s_{ki} is the reactant stoichiometric coefficient of component i in reaction k. In expression (3.22), H_{rk} is the enthalpy of reaction k. In (3.15), H_j was mentioned to be the energy in a thermodynamic system. That is what enthalpy describes. Without going into too much detail, the enthalpy of a system is the internal energy of said system plus the product of pressure and volume. The internal energy is the energy required to create a system. The same energy needs to be made room for and therefore displaces the environment and has a certain pressure and volume. The enthalpy can also be equated to the total heat content of a system and can be written on the form:

$$H = U + pV \qquad (4.23) \quad [30]$$

In equation (3.23), U is the internal energy of the system. p denotes the pressure of the system and V is the volume of said system.
r_k in (3.21) and (3.22) is the volumetric rate of reaction k. This rate is calculated using a model of reaction kinetics. However, which particular model was used is not stated in the STARS guide.

The STARS simulator also takes into consideration a heat loss source/sink term for energy:

$$\sum_{k=1}^{n_r} HL_k + HL_v + HL_c \qquad (4.24) \quad [25]$$

In expression (3.24), HL_k is the heat transfer rate from block face k to the region of interest. The heat is transferring to the adjacent formation. The heat may also be transferred from the adjacent formation to the reservoir. The heat transfer rate uses an analytical model which assumes an infinite overburden formation. This approach eases the heat transfer calculations for the intended purpose. Analytical models are usually easier to solve than empirical models. In the analytical models, one can make certain assumptions and the models may represent ideal scenarios. The empirical models require field data and, ultimately, the results between the two models may not differ significantly.
HL_v represents the heat transfer rate caused by convection. HL_c is a constant heat transfer model.

The phase fractions w_i, x_i, y_i, or more specifically the phase mole fractions, are expressed using equilibrium ratios:

$$y_i = K_i^{go} x_i \quad ; \qquad x_i = K_i^{og} y_i$$

$$x_i = K_i^{ow} w_i \quad ; \qquad w_i = K_i^{wo} x_i$$

$$w_i = K_i^{wg} y_i \quad ; \qquad y_i = K_i^{gw} w_i \qquad\qquad (4.25) \quad [25]$$

In the equations stated under (3.25), the equilibrium ratios, or K values, for component i will have different values between the different phases. For instance, the equilibrium ratio between gas and oil, K_i^{go}, will differ from the equilibrium ratio between oil and water, K_i^{ow}.

There also exist constraints put on the phase mole fractions:

$$\sum_{i=1}^{n_c} y_i = 1 \quad \text{when} \quad S_g > 0 \qquad\qquad (4.27) \quad [25]$$

$$\sum_{i=1}^{n_c} x_i = 1 \quad \text{when} \quad S_o > 0 \qquad\qquad (4.28) \quad [25]$$

$$\sum_{i=1}^{n_c} w_i = 1 \quad \text{when} \quad S_w > 0 \qquad\qquad (4.29) \quad [25]$$

For instance, if the gas saturation in the fluid of interest has a gas saturation higher than 0, the mole fraction of gas in said fluid, if all gas components are added up, will be equal to 1.

The pressure constraints put on the phases are as follows:

$$p_w = p_o - p_{cow}(S_w)$$

$$p_g = p_o + p_{cog}(S_g) \qquad\qquad (4.30) \quad [25]$$

From the equations under (3.30), the water pressure is dependent on difference between the oil pressure and an oil-water pressure that is a function of water saturation. The gas pressure is dependent on the sum of the oil pressure and an oil-gas pressure that is a function of gas saturation.

Finally, there are well equations for the volumetric well phase rates, q_{jk}, discussed in equation (3.18). The operating conditions, chosen by the user of the STARS simulator, put constraints on the well equations. Also mentioned in equation (3.18), is the index I_{jk} which may contain the mobility factor $\left(\frac{k_{rj}}{\mu_j}\right)$. The mobility factor makes the well equations be closely coupled with reservoir conditions. For this reason, the well equations should be solved simultaneously with the conservation equations.
For both the injection wells and production wells, the following equations pertain for constant water-, oil-, gas-, liquid- and steam production rate, respectively:

$$\sum_{k=1}^{n_{lay}} q_{wk} = q_{spec} \qquad\qquad (4.31) \quad [25]$$

$$\sum_{k=1}^{n_{lay}} q_{ok} = q_{spec} \qquad\qquad (4.32) \quad [25]$$

$$\sum_{k=1}^{n_{lay}} q_{gk} = q_{spec} \qquad\qquad (4.33) \quad [25]$$

$$\sum_{k=1}^{n_{lay}} (q_{wk} + q_{ok}) = q_{spec} \qquad\qquad (4.34) \quad [25]$$

$$\frac{1}{\rho_w^{ST}} \{\sum_{k=1}^{n_{lay}} q_{gk} y_1 \rho_g\} = q_{spec} \qquad\qquad (4.35) \quad [25]$$

In the equations above, (3.31) through (3.35), q_{spec} is the quantity that is specified by the user. This quantity is a constant, however, the distribution of fluid to the different layers depends on I_{jk} which can change over time.

Constant pressure is specified in the following way:

$$p_{wf} = p_{spec} \qquad\qquad (4.36) \quad [25]$$

Equations (3.31) through (3.35), as mentioned before, are solved simultaneously with the conservation equations and p_{wf} serves as an additional variable.
In equation (3.35), ρ_w^{ST} is the density of the steam in the steam production rate. $q_{gk} y_1 \rho_g$ is the mole rate, and y_1 and ρ_g are values taken from the grid block containing well layer k. The rates specified in equations (3.31) through (3.35) uses surface conditions. Production wells, however, may use rates that are linked to the reservoir, or at the bottom of the production well.

The wellbore pressure has to be calculated for each well layer k. To that end, an equation analogous to the topic of hydrostatic pressure discussed in chapter 1, under 'Carbonated brine and physics', is employed:

$$p_{wfk} = p_{wf} + \int_{h_1}^{h_k} \gamma_{av} g dh \qquad\qquad (4.37) \quad [25]$$

The integral taken over dh makes up the accumulated pressure head that comes from the elevation of well layer k. γ_{av} is the average mass density of the fluid in the wellbore.

The terms for flowing component i, (3.10), (3.13), (3.14), (3.16), (3.19) and (3.21), may be added together to form the conservation equation:

$$\frac{\partial}{\partial t} \left[V_f (\rho_w S_w w_i + \rho_o S_o y_i + \rho_g S_g x_i) + V_v A d_i \right]$$

$$= \sum_{k=1}^{n_f} [T_w \rho_w w_i \Delta \Phi_w + T_o \rho_o x_i \Delta \Phi_o + T_g \rho_g y_i \Delta \Phi_g] + V \sum_{k=1}^{n_r} (s'_{ki} - s_{ki}) r_k$$

$$+ \sum_{k=1}^{n_f} [\phi \rho_w D_{wi} \Delta w_i + \phi \rho_o D_{oi} \Delta x_i + \phi \rho_g D_{gi} \Delta y_i] + \delta_{iw} \sum_{k=1}^{n_f} \rho_w q a q_{wk}$$

$$+ \rho_w q_{wk} w_i + \rho_o q_{ok} x_i + \rho_g q_{gk} y_i \qquad\qquad (4.38) \quad [25]$$

The equation (3.38) pertains to well layer k. n_f is the number of neighboring regions to the grid block of interest.

The conservation equation for the solid components can be written similarly by adding together the terms (3.11) and (3.21). (3.21) is valid for flowing- and solid component i as chemical interactions are happening in both cases:

$$\frac{\partial}{\partial t}[V_v c_i] = V \sum_{k=1}^{n_r}(s'_{ki} - s_{ki})r_k \qquad\qquad (4.39) \quad [25]$$

For energy, the conservation equation can expressed by adding together the terms (3.12), (3.15), (3.17), (3.20), (3.22) and (3.24):

$$\frac{\partial}{\partial t}\left[V_f\left(\rho_w S_w U_w + \rho_o S_o U_o + \rho_g S_g U_g\right) + V_v c_s U_s + V_r U_r\right]$$

$$= \sum_{k=1}^{n_f}[T_w \rho_w H_w \Delta\Phi_w + T_o \rho_o H_o \Delta\Phi_o + T_g \rho_g H_g \Delta\Phi_g] + \sum_{k=1}^{n_f} K\Delta T$$

$$+ \rho_w q_{wk} H_w + \rho_o q_{ok} H_o + \rho_g q_{gk} H_g + V \sum_{k=1}^{n_r} H_{rk} r_k$$

$$+ \sum_{k=1}^{n_r} HL_k + HL_v + HL_c + \sum_{k=1}^{n_f}(HA_{CV} + HA_{CD})_k \qquad\qquad (4.40)$$

In the STARS user guide, $\sum_{k=1}^{n_r} HL_k$ has been replaced by HL_o which I believe, although it is not stated in the guide, represents the 'overall' heat loss, or HL for each layer k added together and renamed HL_o. Equations (3.38) and (3.40) are spatially discretized. Discretization of continuous functions help solve them numerically. If looking at reservoir flow from left to right, the fluid state at a certain point may be determined by looking at the difference between its state just before and after said point. When considering a point j, or block j, in a reservoir model, spatial discretization makes use of the difference point $j + 1$ and $j - 1$ to determine the fluid state at point j. Similarly, the fluid values at point $j + 1$ may be determined by the difference between point $j + \frac{3}{2}$ and $j + \frac{1}{2}$. Point $j - 1$ may be represented by $j - \frac{1}{2}$ and $j - \frac{3}{2}$.

4.2 Towards the surface

In the SPE paper "Coupled Carbon Dioxide Sequestration and Energy Production From Geopressured/Geothermal Aquifers" reviewed in chapter 2, Ganjdanesh et. al. assumed a producing fluid temperature of 300°F. The STARS simulator models heat flow inside the reservoir. However, the producing fluid's journey towards the surface warrants some discussion as it is coupled with energy exploitation potential.

When the produced fluid reaches the surface with a certain temperature, its heat may be exploited through the use of turbines. The Carnot cycle is one way of expressing energy conversion efficiency:

$$\eta = 1 - \frac{T_L}{T_H}$$
(4.41)   [31]

In equation (3.41), η denotes the efficiency of the energy conversion. T_L and T_H denote the outlet and inlet temperatures of the fluid, respectively. However, it was found that a more realistic approach to determining the energy conversion efficiency was achieved by using the Chambadal-Novikov efficiency:

$$\eta_{CA} = 1 - \sqrt{\frac{T_L}{T_H}}$$
(4.42)   [32]

Using the Curzon-Ahlborn cycle will yield a lower efficiency. It may also be observed that higher inlet temperatures yield higher conversion efficiencies. Equation (3.42) describes the potential energy that may be extracted from a fluid once it has reached the surface. The heat transfer interactions a fluid experiences on its way towards the surface include convective- and conductive heat transfer. The producing fluid will have a certain temperature differential compared to the casing, cement and formation it is travelling along. This temperature differential causes convection. Because the casing, cement and formation are not 100% isolating, a conductive heat transfer will happen that causes the producing fluid to lose heat. Conductive heat transfer rate may be expressed by Fourier's law:

$$q = -k\nabla T = -kA\frac{\Delta T}{L}$$
(4.43)   [33]

In equation (3.43), denotes q the heat flow, A is the total cross-sectional area on which the heat transfer is taking place, k denotes the conductivity of the material the fluid is losing heat to. ∇T is the temperature gradient of the formation. Similar to the pressure gradient discussed in chapter 1, a temperature gradient exists in the earth's crust. The convection that happens inside the wellbore, causes the heated fluid to constantly make contact with the cooler casing surface, ultimately causing a conductive heat loss to the formation. The heat transfer due to convection may be expressed by Newton's law of cooling:

$$q_s = hA(T_s - T_f) = hA\Delta T$$
(4.44)   [33]

In equation (3.44), q_s is the heat flux at the surface, h is a heat transfer coefficient, A is the surface area where convection is taking place. ΔT is the difference in temperature between the solid surface and the initial fluid temperature. The convection heat transfer happens as a fluid moves along a surface, however, there is no fluid movement at the surface itself. At the surface, heat is transferred by conduction, and it may be seen that equation (3.44) is derived from Fourier's law.
The casing in which the fluid is flowing, makes up a cylindrical shape. The convective heat transfer may

therefore be expressed as:

$$q_s = h2\pi r_i L (T_s - T_f)$$ (4.45)

The index i references the inside of the casing diameter. L is the length of the casing. The conductive heat that transfers through the casing may be expressed as:

$$q = -k2\pi r L \frac{dT}{dr}$$ (4.46)

In equation (3.46), the thickness of the casing, or the material one is considering, will make up the boundaries for which the integral over dr will be taken. The temperature difference will make up the boundaries for which the integral over dT will be taken. If conductive heat transfer is happening between the fluid and the casing, one can solve equation (3.46) and merge it with (3.45):

$$\int_{T_f}^{T_n} dT = -\left(\frac{q}{2\pi L k}\right) \int_{r_i}^{r_o} \frac{dr}{r}$$ (4.47)

The index o references the outside of the casing. T_n is a new temperature. Adding equation (3.45) yields:

$$T_f - T_n = \frac{q}{2\pi L} \left(\frac{\ln\left(\frac{r_o}{r_i}\right)}{k} + \frac{1}{r_i h} \right)$$ (4.48)

If one expresses the overall heat loss as:

$$q = UA\Delta T = U2\pi r_i L (T_f - T_n)$$ (4.49)

One can incorporate this equation with (3.48) and obtain:

$$U = \left(\frac{r_i \ln\left(\frac{r_o}{r_i}\right)}{k} + \frac{1}{h} \right)^{-1}$$ (4.50)

In equation (3.50), U is the overall heat transfer coefficient and k is the casing's thermal conductivity. Looking at equation (3.50), one can infer that a small k value will minimize the heat losses [34]. Casing material selection is important for the energy recovery potential when extracting geothermal fluid.

Using a Ph.D. thesis written by Eirik Kårstad in 1999, titled "Time-Dependent Temperature Behavior in Rock and Borehole", Mesfin A. Belayneh was able to adapt an equation to solve for the fluid temperature at the surface:

$$T_{fm} = T_p + B\frac{dT_p}{dz} + \Delta T_{fric} + hz(T_{fm} - T_p)$$ (4.51)   [35]

Where,

$$B = \frac{w c_{fl}}{2\pi r_d U_d}$$ (4.52)   [35]

In equation (3.51), T_{fm} is the formation temperature, T_p is the fluid temperature, z is the depth of the pipe in the well that is producing fluid and h is the heat capacity of the said pipe. In equation (3.52), w is the mass flow rate, c_{fl} is the heat capacity of the producing fluid, r_d is the pipe radius and U_d is the thermal conductivity of that pipe.

The formation temperature is dependent on the temperature gradient of the formation and be expressed as:

$$T_{fm} = T_{surf} + Gz$$ (4.53)   [35]

In equation (3.53), T_{surf} is the surface temperature and G denotes the geothermal gradient. Equation (3.51) can together with (3.53) be expressed as:

$$T_{surf} + Gz = T_p + B\frac{dT_p}{dz} + \Delta T_{fric} + hz\left((T_{surf} + Gz) - T_p\right)$$ (4.54)   [35]

One can obtain a general solution of equation (3.54) by taking the integral:

$$T_p = Ce^{-\frac{z}{B}}T_p + \frac{T_{surf} + Gz - \Delta T_{fric}}{B} - \frac{G}{B^2}$$ (4.55)   [35]

To get the integration constant, C, equation (3.55) may be solved using the so-called initial value problem and setting T_p at the bottom equal to the reservoir temperature, T_{bot}. At the bottom, z is equal to z_{bot}:

$$C = \left(T_{bot} - \frac{T_{surf} + Gz_{bot} - \Delta T_{fric}}{B} + \frac{G}{B^2}\right)e^{\frac{z_{bot}}{B}}$$ (4.56)   [35]

Equation (3.56) may finally be inserted into equation (3.55) and yields:

$$T_p = \left(T_{bot} - \frac{T_{surf} + Gz_{bot} - \Delta T_{fric}}{B} + \frac{G}{B^2}\right)e^{\frac{z - z_{bot}}{B}} + \frac{T_{surf} + Gz - \Delta T_{fric}}{B} - \frac{G}{B^2}$$ (4.57)

[35]

Looking at the aim of this thesis, assuming certain fluid temperatures is sufficient. The aim here, is to look at different well configurations to see if certain configurations opt for better energy recovery. The principles of well configurations stay the same whether or not the drillpipe is insulated. However, the heat interactions between the aquifer and the surface must be considered if an extensive study is to be done on the energy recovery potential.

4.3   Simulating different well placements

To carry out the objective of this thesis, a base case needed to be built in the simulator. The values and parameters regarding the deep saline aquifer were based on the aquifer model from 'Coupled Carbon Dioxide Sequestration and Energy Production from Geopressured/Geothermal Aquifers' [3]. Additionally, some values were given by my assistant supervisor, Alireza Zare:

Table 4.1: Properties of unit cell for saline aquifer

Length, ft	10 560
Width, ft	900
Thickness, ft	300
Number of gridblocks	80*1*30
Gridblock size	132*900*10
Depth at top of the formation, ft	15 000
Temperature, °F	302
Initial pressure, psi	11 000
Salinity, ppm	100 000
Porosity, %	0.2
Horizontal permeability, md	200
Vertical permeability, md	20
Gas mole fraction CH_4	0.0037947
Water mole fraction H_2O	0.996205

The reason for using 1 block in width has to do with a STARS licensing limitation. The first intention was to build a reservoir model scaled equally in the I and J direction. In the simulator, I and J make up the horizontal plane of the reservoir, and K makes up the vertical direction of the reservoir.

To incorporate the thermal properties of the aquifer, the following values, based on work done by Alireza Zare, were used:

Table 4.2: Thermal rocktypes (aquifer)

Porosity reference pressure, psi	11 000
Formation compressibility, 1/psi	$3.0*10^{-6}$
VHC* aquifer, Btu/(ft^{3o}F)	1.866
VHC overburden, Btu/(ft^{3o}F)	1.866
VHC underburden, Btu/(ft^{3o}F)	1.866
TC** overburden, Btu/(ft°F*day)	1.255
TC underburden, Btu/(ft°F*day)	1.255
TC oil, Btu/(ft°F*day)	5.640
TC water phase, Btu/(ft°F*day)	0.457
TC oil phase, Btu/(ft°F*day)	0.0983
TC gas phase, Btu/(ft°F*day)	$1.196*10^{-3}$
* VHC = Volumetric heat capacity, ** TC = Thermal conductivity	

For the reservoir fluid components and the components to be injected, the following parameters were used, also based on the values from 'Coupled Carbon Dioxide Sequestration and Energy Production from Geopressured/Geothermal Aquifers' [3]:

Table 4.3: Component properties

	CO_2	CH_4	H_2O
Critical pressure, psi	1070	667.2	3198
Critical temperature, °F	87.89	-116.59	706.470
Critical volume, ft^3/lbmol	1.505	1.586	0.8970
Molecular weight, lb/lbmol	44.01	16.043	18.015
KV1, psi			$1.7202*10^6$
KV4, °F			-6869.590
KV5, °F			-376.640
Liquid phase viscosity			0.1702

KV1, KV4 and KV5 are K-values calculated using the STARS guide. Critical temperatures and critical pressures were gathered from the STARS guide [25].

The values for the relative permeability curves were based on the values found in from 'Coupled Carbon Dioxide Sequestration and Energy Production from Geopressured/Geothermal Aquifers' [3]. Although, since there is assumed to be no initial or residual oil in the aquifer, $S_o = 0$. The relative permeabilites regarding oil are therefore arbitrary values and have no effect on the outcome of the simulator runs.

Table 4.4: Relative permeability in a water-wet aquifer

S_w	K_{rg}	K_{rw}	k_{row}	k_{rog}
0.200	0.650	0.000	1.000	0.000
0.250	0.550	0.005	0.830	0.005
0.300	0.470	0.010	0.670	0.010
0.350	0.390	0.015	0.540	0.015
0.400	0.320	0.020	0.420	0.020
0.450	0.260	0.040	0.320	0.040
0.500	0.200	0.060	0.240	0.060
0.550	0.160	0.080	0.180	0.080
0.600	0.110	0.120	0.120	0.120
0.650	0.080	0.180	0.080	0.180
0.700	0.060	0.240	0.060	0.240
0.750	0.040	0.320	0.040	0.320
0.800	0.020	0.420	0.020	0.420
0.850	0.010	0.540	0.015	0.540
0.900	0.000	0.670	0.010	0.670
0.950	0.000	0.830	0.005	0.830
1.000	0.000	1.000	0.000	1.000

The last step in developing the base case was to create a vertical injection well. For the injector to be operative, certain constraints needed to be put on the well. The bottomhole pressure was set to 12 000psi. The surface phase injection rate was set to 10 000bbl/day. The injected fluid-pressure was set to 12 000psi with a temperature of 68°F. The mole fractions of the injected fluid were set to 0.9778648 and 0.0221352 for water and CO_2, respectively. With time-steps of 0.001day, the simulator was set to run over a time period of 20 years, or 7300 days. The time period could have been shorter, or longer, but the most important objective of this thesis is to study the effect of well placement compared to CO_2-storing efficiency. The parameters chosen for the injection well were based on 'Coupled Carbon Dioxide Sequestration and Energy Production from Geopressured/Geothermal Aquifers' [3].

4.4   Assumptions and shortcomings of the aquifer model

In the simulator, the formation blocks outside the aquifer are non-existent. Flow is therefore only possible inside the aquifer boundaries. This constraint also forces the fluid flow in the aquifer to be from left to right if the injection well is placed alongside the left aquifer boundary. One could consider the boundaries of the aquifer to be an impermeable formation, making flow inside the boundaries to be a path of least resistance for the injected fluid.

The values of all the parameters put into the simulator are the results of extensive studies done on the subject of CO_2-sequestration. Additionally, not all parameters required to represent a realistic scenario were available. Therefore, a stunted representation of the production data are reflected in the simulation runs. However, limitations included, the principles behind well placements and their impact should remain intact.

4.5   Results

In the first scenario, a simple vertical injector and producer are simulated. A bottomhole pressure constraint of 11 100psi was set on the producer (the pressure constraint was kept the same for all 7 models):
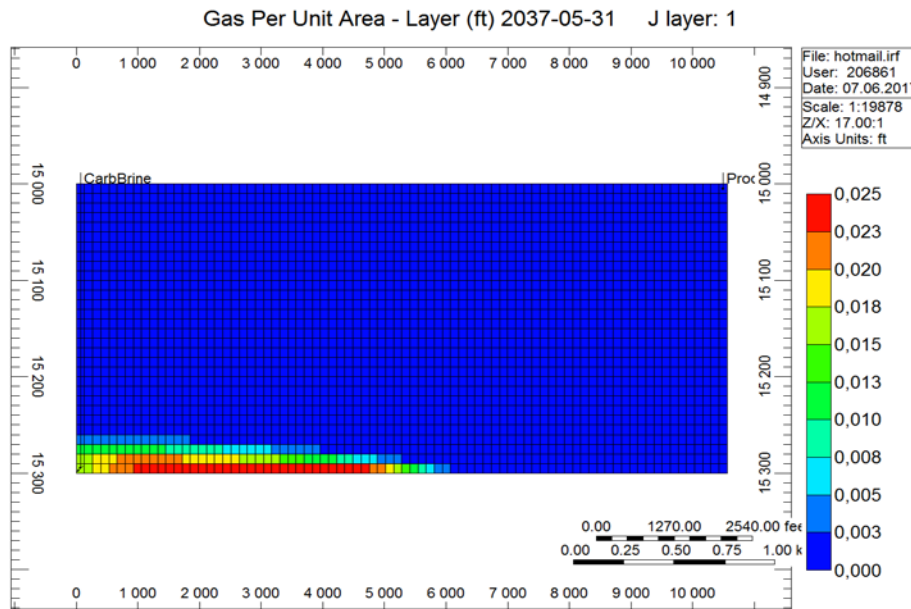

Figure 4.2: Model 1 - Vertical injector perforated in 1 1 30. Vertical producer perforated in 80 1 1.

This first model used a perforation in the bottom left block, or 1 1 30. The displacement is heavily horizontally weighted. The displacement trend is due to the horizontal permeability being 10 times higher than the vertical permeability. The different block colors represent different mole fractions of CO_2.
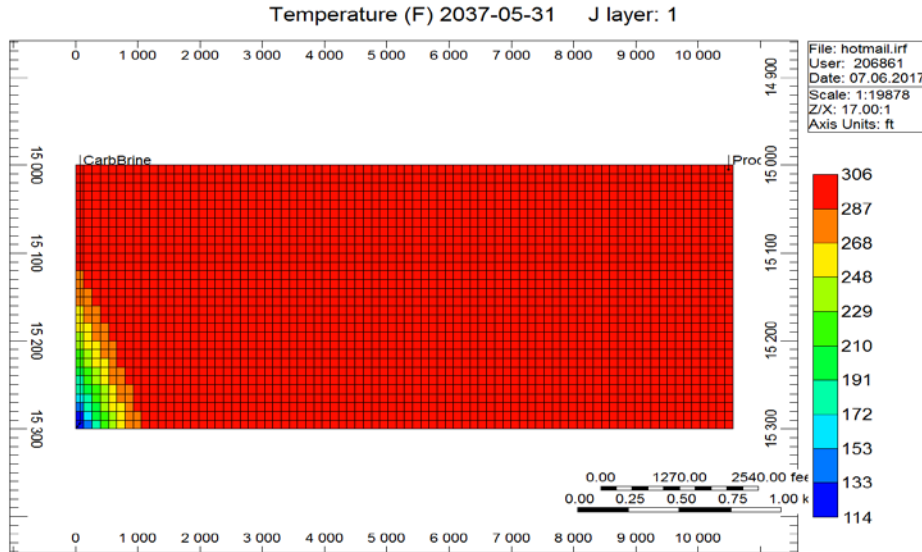
Figure 4.3: Model 1 - Temperature effect on aquifer

The temperature disturbance, assuming this model is correct, is fairly insignificant on an aquifer of this magnitude. After having evened out, the injection rate or Model 1 was 254.1bbl/day and $1.37*10^4 ft^3$/day for water and CO_2, respectively. The production rate of water was 259.4bbl/day.

The second idea was to create a model with a horizontal injection well. The same constraints were kept on the well. The perforation location was changed to 9 1 29. The simulation run showed slightly higher injection rates with 275.6bbl/day and $1.49*10^4 ft^3$/day for water and CO_2, respectively. The production rate of water was 281.5bbl/day for the second model.
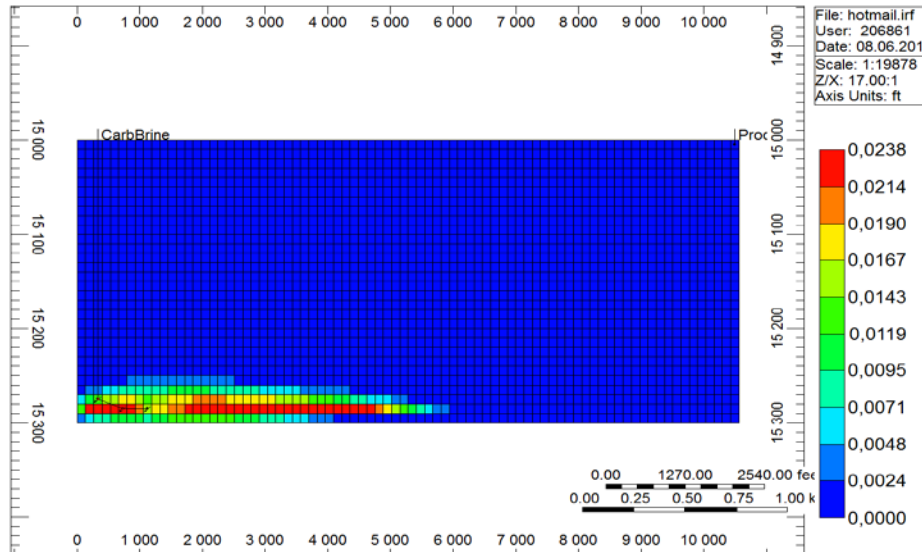

Figure 4.4: Model 2 - Horizontal injector perforated in 9 1 29.

In a third scenario, a slanted well in the upper left corner was investigated. The perforation was set to block 9 1 9. The injection rates increased to 714.7bbl/day and $3.87*10^4 ft^3$/day for water and CO_2,

respectively. The production rate saw an increase to 729.3bbl/day. There was a CO_2-breakthrough after 6848 days.
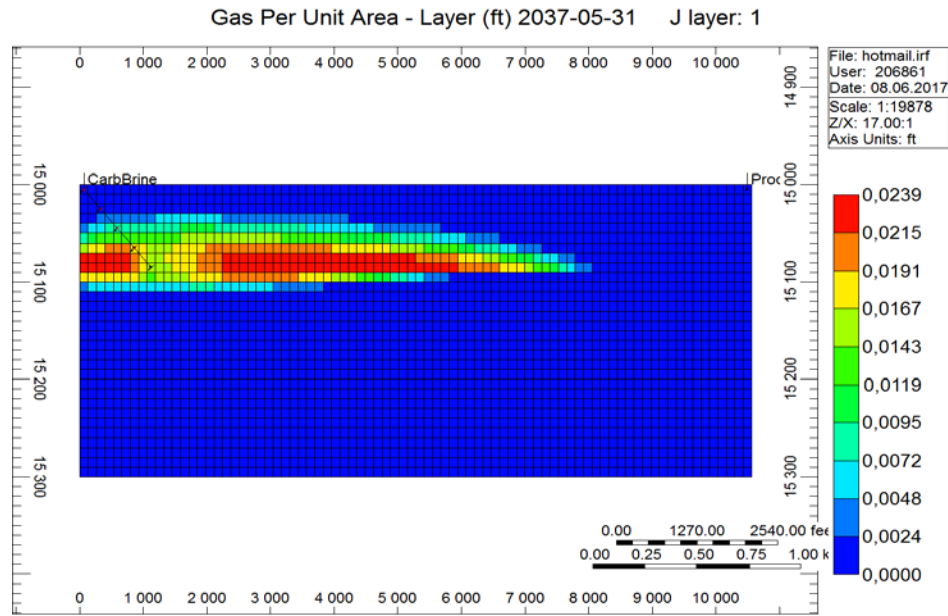

Figure 4.5: Model 3 - Slanted injector perforated in 9 1 9.

In the fourth model, the slanted well was placed in the bottom left corner of the aquifer. The producer was placed in the bottom right corner of the aquifer. At CO_2-breakthrough, the injection rates were 939.0bbl/day and $5.08*10^4 ft^3$/day for water and CO_2, respectively. The CO_2-breakthrough, however, happened after 1826 days. At this time, the production rate of water was 956.4bb/day.
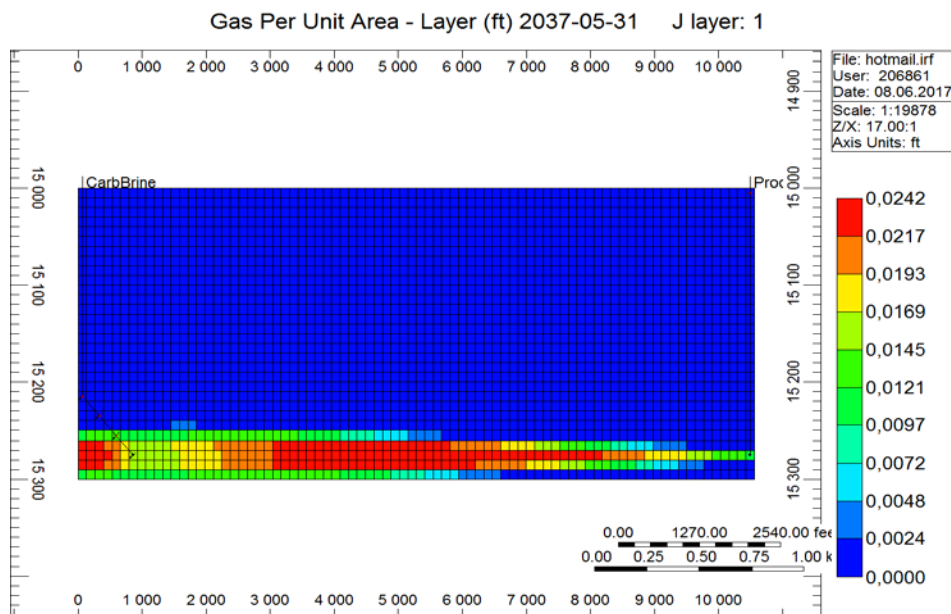

Figure 4.6: Model 4 - Slanted injector perforated in 7 1 28. Vertical producer perforated in 80 1 28.

In Model 5, a slanted injection well was placed in the upper right corner with perforations in 9 1 9. The producer was kept in the same position as in Model 4. This scenario gave injection rates of 394.9bbl/day and $2.13*10^4$ft^3/day for water and CO_2, respectively. The production rate of water was 403.0bbl/day. There was no CO_2-breakthrough in Model 5.

Model 6 tried a slanted producer in the upper right corner with perforations in 76 1 5. There was no CO_2-breakthrough. The injection rates were 329.8bbl/day and $1.78*10^4$ft^3/day for water and CO_2, respectively. The production rate of water was 336.6bbl/day.

In the seventh model, the injector was set in the bottom left corner, horizontally, with perforations in 9 1 29. The producer was placed to the right in the aquifer with perforations in 80 1 15. The injection rates were 496.0bbl/day and $2.68*10^4$ft^3/day for water and CO_2, respectively. The production rate of water was 506.1bbl/day with no CO_2-breakthrough.

Table 4.5: Data summary for simulation models

	Injection rate H_2O, bbl/day	Injection rate CO_2, ft^3/day	Production rate H_2O, bbl/day	CO_2-breakthrough, day
Model 1	254.1	1.37	259.4	No
Model 2	275.6	1.49	281.5	No
Model 3	714.7	3.87	729.3	6848
Model 4	939.0	5.08	956.4	1826
Model 5	394.9	2.13	403.0	No
Model 6	329.8	1.78	336.6	No
Model 7	496.0	2.68	506.1	No
Model 8	809.0	4.38	825.5	5936

Model 8 was made for the purpose of figure 5.1 in the discussion section.

5   Discussion

Looking at a deep saline aquifer with dimensions similar to those of Model 1 through Model 7, the temperature disturbance in the aquifer seemed rather inconsequential. This bodes well for the energy recovery potential – there will be no reduction in produced fluid temperature before CO_2-breakthrough.

The difference between the use of vertical-, horizontal- and slanted wells appeared, more or less, insignificant. The most influential factors regarding CO_2-breakthrough and injection- and production rates seemed to be the vertical- and horizontal distance differentials between the injector and producer. Increasing the horizontal- and vertical permeability made the breakthrough happen earlier, as one would expect. The vertical- to horizontal permeability ratio was kept the same.
Looking at Model 1, Model 4 and Model 7, the injection- and production rates are approximately proportional to the depth differential between the producer and injector, reflecting the vertical- to horizontal permeability ratio.
If one approximates the horizontal distance differentials of Model 1, Model 4 and Model 7 to 80 blocks, the injection- and production rates approximately double as the depth differential is decreased by 15 blocks.
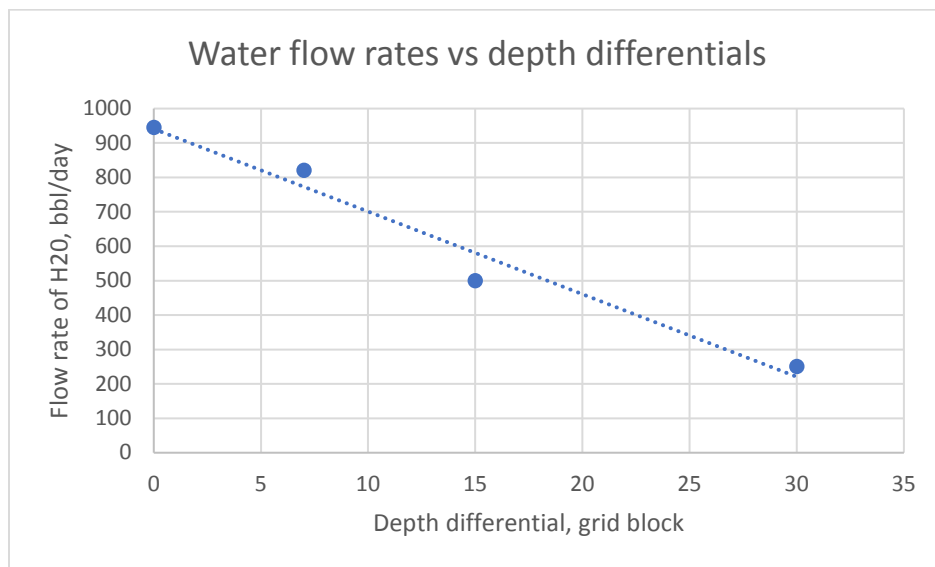

Figure 5.1: Showing a linear relationship between depth differential between wells with H2O flow rates (approximate values are represented).

The pressure drawdown effect created by the production well appears to register more heavily when the injector and producer are aligned horizontally. This makes sense because the horizontal permeability is 10 times that of the vertical permeability – the connection is better. Horizontally aligned wells can therefore have higher flow rates while maintaining material balance and the reservoir pressure.

According to the aquifer model used in these simulation runs, the CO_2-breakthrough time may be described as a function of aquifer flow rates. The aquifer flow rates in turn, are dependent on the vertical- to horizontal permeability ratio and the vertical- and horizontal distance differentials.

$$Q_{aq} = f\left(\frac{k_v}{k_h}, d\right) \tag{3.55}$$

In equation (3.55), Q_{aq} is aquifer flow rate. The right-hand side of (3.55) shows some function, f, dependent on the distance, d, between the injector and producer and the permeability ratio, $\frac{k_v}{k_h}$. Because the fluid being injected into the aquifer is described by mole fractions, a higher flow rate of water means a higher rate of CO_2.

The pressure drawdown, p_{dd}, would depend on both the distance and the vertical- to horizontal permeability ratio. Equation (3.55) may then be rewritten as:

$$Q_{aq} = p_{dd}\left(\frac{k_v}{k_h}, d\right) \tag{3.56}$$

The distance between injector and producer may be seen as a right triangle. Well logs can be used to measure well positions. In a three-dimensional reservoir, the distance between injector and producer may be expressed as:

$$d = \sqrt{(x_p - x_i)^2 + (y_p - y_i)^2 + (z_p - z_i)^2} \tag{3.57}$$

In equation (3.57), x and y describe the horizontal positions of the wells and z is their vertical positions. Ultimately, the CO_2-breakthrough time may be expressed as some general function, g, of flow rate:

$$N_{gas} = g\left(Q_{aq}\right) \tag{3.58}$$

In equation (3.58), N_{gas} is the number of days before gas-breakthrough.

The optimal scenario would be to have the flow rates be as high as possible without an early gas-breakthrough. Slower injection rates means higher operational costs, so one would have to weigh costs against the potential amount of CO_2 that could be stored. To find the exact depth differential that cause the highest injection rates for a given reservoir with late gas-breakthrough, further studies with more detailed aquifer models should be investigated. Furthermore, varying aquifer size and -properties could produce additional insight in ascertaining the optimal depth differential of injector and producer placement.

6 Conclusion

The CMG STARS simulator was used to explore the impact of well configuration on dissolved CO_2 storing in a deep saline aquifer. The method of injecting dissolved CO_2 versus a supercritical version of the gas shows to be a promising option. Injecting dissolved CO_2 and simultaneously extracting the aquifer brine limits reservoir disturbance and yields a substantial energy recovery. The recovered fluid may be exploited for its heat and gas content to negate the energy consumption required for CCS. The cooling effect of the injected fluid on the aquifer seemed of little significance. The simulation models showed a clear correlation between amount of CO_2 stored and well placement. Distance between the injection well and the production well became the most dominant factor regarding CO_2-breakthrough time. Furthermore, the vertical distance between wells played a significant role due to the vertical- to horizontal permeability ratio – the horizontal permeability being 10 times higher than the vertical permeability. Because the injected brine had an almost similar density to the aquifer brine, injection rates highly echoed production rates. The most optimal solution regarding well placement would be to find the point at which injection rates are as high as possible without having an early CO_2-breakthrough. Aquifer sizes vary and well placement will have to follow accordingly.

Directions for future work: (1) discovering more accurate correlations between well placement and CO_2-storing efficiency by using more detailed models for simulation studies; (2) exploring the effect of aquifer heterogeneity on well placement optimization; (3) implementing faults in both homogeneous- and heterogeneous aquifers to see their effect on well placement.

Appendix

Polytropic equation:

$$\dot{W}_{CO_2} = \frac{S\dot{N}_{CO_2}nRT_1}{(n-1)}\left(\left(\frac{P_{mixing}}{P_1}\right)^{\frac{n-1}{nS}} - 1\right) \qquad \text{(A.1)} \quad [2]$$

S is the number of compressor stages (10) and the polytropic constant n is calculated by

$$n = \frac{k\eta_p}{1+k\eta_p-k} \qquad \text{(A.2)} \quad [2]$$

η_p is the poytropic efficiency (80%) and k is the ratio of specific heats for CO_2 (1.30).

Mechanical energy balance:

$$\dot{W}_{Brine} = \frac{q_{Brine}(P_{mixing}-P_1)}{\eta_{pump}} \qquad \text{(A.3)} \quad [2]$$

In (3.62) η_{pump} is set to 80%.

Thermal efficiency of ORC:

$$\eta_{th} = \frac{\dot{W}}{\dot{Q}} = 0.0935T(°C) - 2.3266 \qquad \text{(A.4)} \quad [2]$$

Corey's equations:

$$k_{rg} = k_{rg}^{\circ}\left(\frac{S_g-S_{gr}}{1-S_{wirr}-S_{gr}}\right)^{n_g} \qquad \text{(A.5)} \quad [3]$$

$$k_{rw} = k_{rw}^{\circ} \left(\frac{S_w - S_{wirr}}{1 - S_{wirr} - S_{gr}} \right)^{n_w} \qquad \text{(A.6)} \quad [3]$$

S_{wirr} is irreducible water saturation and S_{gr} is residual gas saturation. k_{rg}° and k_{rw}° are endpoint relative permeabilities for gas and water, respectively. n_g and n_w are the Corey exponents for gas and water, respectively.

Land's equations:

$$k_{rg} = k_{rg}^{\circ} \left(\frac{S_g(shifted) - S_{gr}}{1 - S_{wirr} - S_{gr}} \right)^{n_g} \qquad \text{(A.7)} \quad [3]$$

$$S_g(shifted) = S_{gr} + \frac{(S_g - S_{grh})(S_{gh} - S_{gr})}{(S_{gh} - S_{grh})} \qquad \text{(A.8)} \quad [3]$$

S_{gh} is the value of S_g when the shift to imbibition occurs. S_{grh} can be calculated from:

$$\frac{1}{S_{gr}^{max} - S_{gr}} - \frac{1}{S_g^{max} - S_g} = \frac{1}{S_{grh} - S_{gr}} - \frac{1}{S_{gh} - S_{gr}} \qquad \text{(A.9)} \quad [3]$$

7 References

[1] M. H. Stephenson, Returning Carbon to Nature: Coal, Carbon Capture, and Storage, Waltham: Eliesevier, 2013.

[2] R. Ganjdanesh, B. S. L, G. A. Pope and K. Sepehrnoori, "Integrating Carbon Capture and Storage with Energy Production from Saline Aquifers: A Strategy to Offset the Energy Cost of CCS," *Energy Procedia,* vol. 63, pp. 7349-7358, 2014.

[3] R. Ganjdanesh, B. S. L, R. L. Orbach, G. A. Pope and K. Sepehrnoori, "Coupled Carbon Dioxide Sequestration and Energy Production From Geopressured/ Geothermal Aquifers," vol. 19, no. 02, pp. 239-248, 2014.

[4] P. E. Eke, M. Naylor, S. Haszeldine and A. Curtis, "CO2-Brine Surface Dissolution and Injection: CO2 Storage Enhancement," in *SPE Offshore Europe Oil & Gas Conference & Exhibition* , Aberdeen, 2009.

[5] The American Society of Mechanical Engineers, "Boiler and Pressure Vessel Code," The American Society of Mechanical Engineers, 2017. [Online]. Available: https://www.asme.org/shop/standards/new-releases/boiler-pressure-vessel-code-2013.

[6] Ikon Science members, "Solutions , Drilling & completions," Ikon Science, 2017. [Online]. Available: https://www.ikonscience.com/solutions/drilling. [Accessed 2017].

[7] B. S. Aadøny, Modern Well Design: second edition, London: Taylor & Francis Group, 2010.

[8] U.S. Energy Information Administration , "Trends in U.S. Oil and Natural Gas Upstream Costs," Independent Statistics & Analysis , Washington, 2016.

[9] Wikipedia contributors, "Hydrocarbon," Wikipedia, 6 March 2017. [Online]. Available: https://en.wikipedia.org/w/index.php?title=Special:CiteThisPage&page=Hydrocarbon&id=783706766. [Accessed 3 April 2017].

[10] Wikipedia contributors, "Petroleum," Wikipedia, 6 June 2017. [Online]. Available: https://en.wikipedia.org/wiki/Petroleum#Crude_oil. [Accessed 1 April 2017].

[11] Wikipedia contributors, "Sedimentary rock," Wikipedia, 8 December 2016. [Online]. Available: https://en.wikipedia.org/wiki/Sedimentary_rock. [Accessed 15 March 2017].

[12] Wikipedia contributors, "Equation of state," Wikipedia, 8 December 2016. [Online]. Available: https://en.wikipedia.org/w/index.php?title=Special:CiteThisPage&page=Equation_of_state&id=753714184. [Accessed 15 March 2017].

[13] Wikipedia contributors, "Mole (unit)," Wikipedia, 25 February 2017. [Online]. Available: https://en.wikipedia.org/w/index.php?title=Special:CiteThisPage&page=Mole_%28unit%29&id=783148304. [Accessed 5 March 2017].

[14] Wikipedia contributors, "Isotope," Wikipedia, 10 January 2017. [Online]. Available: https://en.wikipedia.org/w/index.php?title=Special:CiteThisPage&page=Isotope&id=784273567. [Accessed 20 May 2017].

[15] Wikipedia contributors, "Compressibility," Wikipedia, 2 February 2017. [Online]. Available: https://en.wikipedia.org/w/index.php?title=Special:CiteThisPage&page=Compressibility&id=783535259. [Accessed 17 March 2017].

[16] Wikipedia contributors, "Thermodynamic temperature," Wikipedia, 12 May 2017. [Online]. Available: https://en.wikipedia.org/w/index.php?title=Special:CiteThisPage&page=Thermodynamic_temperature&id=780033882. [Accessed 21 May 2017].

[17] Exergy S.p.A, "Organic Rankine Cycle Tecknology," Exergy S.p.A, [Online]. Available: http://exergy-orc.com/technology/orc#. [Accessed 15 May 2017].

[18] Wikipedia contributors, "Molar solubility," Wikipedia, 30 April 2017. [Online]. Available: https://en.wikipedia.org/w/index.php?title=Special:CiteThisPage&page=Molar_solubility&id=777954833. [Accessed 15 May 2017].

[19] Wikipedia contributors, "Permeability (earth sciences)," Wikipedia, 10 March 2017. [Online]. Available: https://en.wikipedia.org/wiki/Permeability_(earth_sciences). [Accessed 22 March 2017].

[20] SPE International, "Capillary pressure," PetroWiki, 10 January 2016. [Online]. Available: http://petrowiki.org/Capillary_pressure. [Accessed 23 March 2017].

[21] Wikipedia contributors, "Relative permeability," Wikipedia, 7 January 2017. [Online]. Available: https://en.wikipedia.org/w/index.php?title=Special:CiteThisPage&page=Relative_permeability&id=784371842. [Accessed 19 March 2017].

[22] SPE International, "Fluid friction," PetroWiki, 4 June 2015. [Online]. Available: http://petrowiki.org/Fluid_friction. [Accessed 7 May 2017].

[23] Wikipedia contributors, "Bernoulli's principle," Wikipedia, 19 December 2016. [Online]. Available: https://en.wikipedia.org/w/index.php?title=Special:CiteThisPage&page=Bernoulli%27s_principle&id=784657612. [Accessed 19 March 2017].

[24] Wikipedia contributors, "British thermal unit," Wikipedia, 9 November 2016. [Online]. Available: https://en.wikipedia.org/w/index.php?title=Special:CiteThisPage&page=British_thermal_unit&id=784416711. [Accessed 12 March 2017].

[25] Computers Modelling Group Ltd., *STARS user guide, advanced processes and thermal reservoir simulator,* CMG Ltd., 2016.

[26] Wikipedia contributors, "Adsorption," Wikipedia, 10 March 2016. [Online]. Available: https://en.wikipedia.org/w/index.php?title=Special:CiteThisPage&page=Adsorption&id=784488495 . [Accessed 15 May 2017].

[27] Schlumberger , "dispersion," Schlumberger Oilfield Glossary, 2017. [Online]. Available: http://www.glossary.oilfield.slb.com/en/Terms/d/dispersion.aspx. [Accessed 5 May 2017].

[28] A.-M. a. Kokal, "Energy Technologies: How They Work and Their Induced Seismicity Potential," in *Induced Seismicity Potential in Energy Recovery*, Washington DC, National Academies Press, 2011, pp. 75-83.

[29] Khan Academy, "Chemical reactions and stoichiometry," Khan Academy , 2017. [Online]. Available: https://www.khanacademy.org/science/chemistry/chemical-reactions-stoichiome#concept-intro. [Accessed 23 March 2017].

[30] Wikipedia contributors, " Enthalpy," Wikipedia , 26 April 2017. [Online]. Available: https://en.wikipedia.org/w/index.php?title=Special:CiteThisPage&page=Enthalpy&id=777350562. [Accessed 3 May 2017].

[31] Wikipedia contributors, " Carnot's theorem (thermodynamics)," Wikipedia, 10 February 2017. [Online]. Available: https://en.wikipedia.org/w/index.php?title=Special:CiteThisPage&page=Carnot%27s_theorem_%28 thermodynamics%29&id=763714484. [Accessed 23 May 2017].

[32] Wikipedia contributors, "Endoreversible thermodynamics," Wikipedia , 7 January 2017. [Online]. Available: https://en.wikipedia.org/w/index.php?title=Special:CiteThisPage&page=Endoreversible_thermodyn amics&id=784384088. [Accessed 7 May 2017].

[33] F. P. Incropera, D. P. DeWitt, T. L. Bergman and A. S. Lavine, Fundamentals of Heat and Mass Transfer, Hoboken: John Wiley & Sons, Inc, 2007.

[34] C. Long and N. Saymar, Heat Transfer, Ventus Publishing ApS, 2009.

[35] M. M. Belayneh, *Simulation of Geothermal System with Convective-Conductive Heat Transfer (Work note),* Stavanger, 2013.